Are direct photons a clean signal of a thermalized quark-gluon plasma?

D. Boyanovsky* and H. J. de Vega†

Department of Physics and Astronomy, University of Pittsburgh, Pittsburgh, Pennsylvania 15260, USA
and LPTHE, Université Pierre et Marie Curie (Paris VI) et Denis Diderot (Paris VII), Tour 16, Premiere Étage,
4 place Jussieu, 75252 Paris Cedex 05, France

Direct photon production from a quark-gluon plasma (QGP) in thermal equilibrium is studied directly in real time. In contrast with the usual S-matrix calculations, the real time approach is valid for a QGP that formed and reached local thermal equilibrium a short time after a collision and of finite lifetime (~ 10–20 fm/c as expected at BNL RHIC or CERN LHC). We point out that during such a finite QGP lifetime the spectrum of emitted photons carries information on the initial state. There is an inherent ambiguity in separating the virtual from the observable photons during the transient evolution of the QGP. We propose a real time formulation to extract the photon yield which includes the initial stage of formation of the QGP parametrized by an effective time scale of formation Γ^{-1}. This formulation coincides with the S-matrix approach in the infinite lifetime limit. It allows us to separate the virtual cloud as well as the observable photons emitted during the preequilibrium stage from the yield during the QGP lifetime. We find that the lowest order contribution $O(\alpha_{em})$ which does *not* contribute to the S-matrix approach, is of the same order of or larger than the S-matrix contribution during the lifetime of the QGP for a typical formation time ~ 1 fm/c. The yield for momenta $\gtrsim 3$ GeV/c features a power law fall-off $\sim T^3 \Gamma^2/k^5$ and is larger than that obtained with the S-matrix for momenta $\geqslant 4$ GeV/c. We provide a comprehensive numerical comparison between the real time and S-matrix yields and study the dynamics of the build-up of the photon cloud and the different contributions to the radiative energy loss. The reliability of the current estimates on photon emission as well as theoretical uncertainties on the details of the initial state are discussed.

I. INTRODUCTION

Amongst the different potential experimental signatures of the formation and evolution of a quark gluon plasma (QGP) that is conjectured to be formed in ultrarelativistic heavy ion collisions, hard electromagnetic probes, namely direct photons and dileptons, are considered to be very promising [1,2]. Photons and dilepton pairs only interact electromagnetically and their mean free paths are much larger than the size of the QGP, thus these electromagnetic probes leave the hot and dense region after formation without further scattering, carrying with them clean information of the early stages of the collision. Therefore a substantial effort has been devoted to obtaining a theoretical assessment of the spectra of direct photons and dileptons emitted from a thermalized QGP [1–9]. Preliminary assessments concluded that direct photon emission from a thermalized QGP can be larger than that from the hadronized phase [3,4], sparking an intense effort to obtain reliable estimates of the direct photon spectrum [5,7,8]. For recent reviews on theoretical and phenomenological aspects of electromagnetic probes, see [10–12].

The first observation of direct photon production in ultrarelativistic heavy ion collisions has been reported by the WA98 Collaboration in ^{208}Pb + ^{208}Pb collisions at $\sqrt{s}$ = 158 GeV at the Super Proton Synchrotron (SPS) at CERN [13]. The results display a clear *excess* of direct photons above the expected background from hadronic decays in the

range of transverse momentum $p_T > 1.5$ GeV/c in the most central collisions. These results provide an experimental confirmation of the feasibility of direct photons as reliable probes in ultrarelativistic heavy ion collisions and may pave the way for understanding the formation and evolution of a QGP.

A variety of fits of theoretical results to the experimental data had been reported [11], however, the results seem inconclusive, models with or without QGP emission seem to fit the data in a manner compatible with models based solely on hadronic "cocktails" (for a detailed review see [11]).

The current ultrarelativistic heavy ion program at the Relativistic Heavy Ion Collider (RHIC-BNL) and the proposed heavy ion program Alice at the forthcoming Large Hadron Collider (LHC-CERN) have as a main goal to continue the experimental pursuit of the long-sought QGP with beam energies of $\sqrt{s} \sim 200$ AGeV for Au + Au at RHIC and up to $\sqrt{s} \sim 5500$ AGeV for Pb + Pb at CERN. This active experimental program with the possibility of statistical analysis on an event-by-event basis justifies the theoretical assessment of experimental probes at a deeper level. For a recent summary of measurements at RHIC see [14].

The S-matrix approach to calculating the photon yield from a QGP in local thermal equilibrium treats the plasma as stationary and with an infinite lifetime, while it is clear that QGP is a transient, nonequilibrium state [15,16]. Current theoretical understanding suggests that a QGP may be formed ~ 1 fm/c after a nucleus-nucleus collision and thermalizes via parton-parton scattering. The subsequent evolution is assumed to be described by hydrodynamic expansion until the

---

*Electronic address: boyan@pitt.edu
†Electronic address: devega@lpthe.jussieu.fr

temperature cools down to the hadronization scale ~ 160 MeV. At RHIC the initial temperature of the plasma is expected to be of the order of 300 MeV, and assuming Bjorken's longitudinal expansion with a cooling law $T(t) = T_i(t_i/t)^{1/3}$ it is expected that the lifetime of the QGP is of order $\lesssim 10$ fm/c for a hadronization temperature of about 160 MeV. At the LHC the initial temperature is expected to reach ~ 450 MeV and the lifetime of the QGP would be expected to be of order $\sim 20-30$ fm/c. The transverse size of the QGP formed in the most central collisions is of the order of the radius of the nucleus which for Pb+Pb is about 7 fm, thus the typical space-time dimension of QGP in local thermal equilibrium is about 10 fm.

Despite the fact that the quark-gluon plasma, if formed, will occupy a finite and rather small volume in space time, the *S*-matrix approach to obtain the photon and dilepton yields treats the plasma as a medium in thermal equilibrium and of infinite extent in space-time [15,16]. The production rate obtained from this approach is then input into a space-time evolution combined with a hydrodynamic expansion of the plasma [10–12]. A recent analysis of photon production along these lines [9] to fit the data from WA98 [13] suggests that the large p_T region is dominated by the first few fm/c of (hydrodynamic) evolution and is very sensitive to the early stages of the evolution.

The issue of a finite space-time extension of the QGP and the hadronic phase has received attention with respect to the emission of photons and dileptons. The influence of a finite *spatial* size of the plasma has been addressed for the emission of thermal photons [17,18] and more recently for thermal dileptons [19] from a hadronic gas, where the breaking of detailed energy-momentum conservation by finite size effects was studied.

Preliminary studies of the finite *lifetime* effects on the photoproduction yield were reported in Ref. [20]. The results of those studies pointed out the importance of nonequilibrium real time processes whose contribution is subleading in the infinite lifetime limit, but that are of the same order or larger than the *S*-matrix contribution during the lifetime of a QGP expected at RHIC and LHC. Two main consequences of the study in Ref. [20] are as follows:

(i) During a finite lifetime the spectrum of direct photons is sensitive to the initial conditions that lead to a thermalized QGP with the large p_T region of the spectrum more sensitive to the initial stages.

(ii) To lowest order α_{em} the spectrum resulting from the nonequilibrium processes flattens for momenta $p_T > 2$ GeV/c. The sensitivity of the large p_T part of the spectrum to initial conditions has also been pointed out in Ref. [9], and perhaps coincidentally, the WA98 data [13] display a flattening of the spectrum for $p_T \gtrsim 1.5$ GeV/c.

The goals of this article are to continue the study of direct photon production from a QGP in local thermodynamic equilibrium with a finite lifetime, directly in real time. We focus on the following aspects:

(i) Assessing the contribution to the direct photon spectrum from the *lowest order* processes that are subleading in the infinite time limit. These processes are $q\bar{q} \to \gamma$ and q $\to q\gamma$ and correspond to the one loop contribution to the photon polarization, namely of order α_{em}. The contributions of these processes vanish in the infinite time limit and do not contribute to the rate obtained from the *S*-matrix approach, but do contribute to the yield during a finite lifetime. Focusing on the lowest order contributions we identify the dynamical aspects of photon production in real time in the simplest possible case. This study highlights that there are contributions to *all orders* in α_s that are being missed by the *S*-matrix calculation.

(ii) A detailed analysis of the dynamics of the build-up of the virtual photon cloud and to provide a systematic effective description of the initial stage between the collision and thermalization that allows a clear separation of the virtual photons. We discuss the inherent difficulties associated with an unambiguous identification of the virtual photon cloud during a finite time interval.

(iii) A systematic description of direct photon production during a finite time interval including the initial preparation of the state.

(iv) An analytic and numerical comparison of the real time yield obtained in lowest order, namely of $O(\alpha_{em})$ and the *S*-matrix yield, of order $\alpha_s \alpha_{em} \ln(1/\alpha_s)$ [7,8] to assess the potential experimental significance of the processes that are missed by the *S*-matrix calculation but that contribute to the direct photon yield from a QGP with a finite lifetime. We provide a comprehensive numerical study of the direct photon yield to lowest order $O(\alpha_{em})$ with an analysis of the spectrum.

(v) A study of the dependence of the spectrum on the initial conditions prior to the onset of local thermal equilibrium. This study reveals important aspects of the initial conditions prior to thermalization that influence the spectrum.

(vi) A study of the radiative energy loss, in particular the contributions associated with the interaction energy as well as the cooling of the plasma by photon emission.

(vii) A simple energy-time uncertainty argument would suggest that for momenta larger than the inverse lifetime of the QGP, the effects of a finite lifetime should be subleading. Our study clearly shows this expectation *not* to bear out. In fact we show that contributions from the region $\omega \neq k$ in the imaginary part of the photon polarization are very important during the finite lifetime and of the same order (or larger) than the usual result valid solely for $\omega = k$ even for photons with large transverse momentum.

This article is organized as follows: in Sec. II we revisit the *S*-matrix approach to highlight its caveats. In Sec. III we present the real time formulation to photon production beginning with a full gauge invariant treatment of the electromagnetic interaction of quarks. In Sec. IV we provide a simple and transparent derivation of the expression for the photon production yield in real time to lowest order in α_{em} and finite QGP lifetime. This formulation reproduces the results obtained in Ref. [20] by a more general kinetic description and is explicitly shown to coincide with the *S*-matrix formulation in the infinite QGP lifetime limit. In this section we address the issue of initial conditions and in particular the subtle but important aspects associated with the formation of the photon cloud. In this section we present a detailed analysis of the

radiative energy loss and the different contributions, providing an analytic and numerical study of the total energy radiated during the lifetime of the QGP. In Sec. V we address the issue of the electromagnetic dressing of the initial state (density matrix) by providing an initial density matrix that includes the photon cloud parametrized by a formation time scale of the QGP after the parton stage following an ultrarelativistic heavy ion collision, conjectured to be ~ 1 fm/c. This parametrization interpolates smoothly between the adiabatic preparation of asymptotic states and the uncorrelated initial state assumed in the S-matrix calculation. The consideration of such initial states (density matrix) allows us to address the issue of the formation time and includes in a phenomenological manner the photon cloud of the preequilibrium stage.

Our conclusions are presented in Sec. VI.

II. S-MATRIX APPROACH AND ITS CAVEATS

In order to highlight the shortcomings of the S-matrix approach to calculate photon emission, and to establish contact with the real-time approach to photon production introduced in Sec. IV, we now summarize some important aspects of the scenario of QGP formation and evolution and the S-matrix approach to the calculation of photon emission.

As mentioned in the Introduction, QGP is conjectured to be formed in ultrarelativistic heavy ion collisions from the deconfinement of strongly interacting quarks and gluons in the incoming nuclei. The details of the dynamics of the collision are not completely understood, nor, in particular, the electromagnetic aspects of the parton distribution functions. It is conjectured that immediately after the collision the partons are almost free and parton-parton scattering leads to a state of (local) thermal equilibrium on a time scale ~ 1 fm/c *after* the collision. The photons emitted during the preequilibrium stage are assumed to leave the medium [24]. The thermalized QGP undergoes adiabatic hydrodynamic expansion during a lifetime of ~ 10–20 fm/c after which the plasma hadronizes. The QGP in local thermal equilibrium under the strong interactions is not in equilibrium under the electromagnetic interactions resulting in photons emitted directly from the thermalized plasma.

The S-matrix approach to the calculation of photon emission begins by writing the Hamiltonian in the form

$$H = H_0 + H_{\text{int}},$$

$$H_0 = H_{\text{QCD}} + H_\gamma,$$

$$H_{\text{int}} = e \int d^3 x J^\mu A_\mu, \qquad (2.1)$$

where H_{QCD} is the full QCD Hamiltonian, H_γ is the free photon Hamiltonian, and H_{int} is the interaction Hamiltonian between quarks and photons with J^μ the quark electromagnetic current, A^μ the photon field, and e the electromagnetic coupling constant.

Consider that at some initial time t_i the state $|i\rangle$ is an eigenstate of H_0 with no photons. The transition amplitude at time t_f to a final state $|f, \gamma_\lambda(\vec{p})\rangle \equiv |f\rangle \otimes |\gamma_\lambda(\vec{p})\rangle$, again an eigenstate of H_0 but with one photon of momentum $\vec{p}$ and polarization λ, is up to an overall phase given by

$$S(t_f, t_i) = \langle f, \gamma_\lambda(\vec{p})| U(t_f, t_i)|i\rangle, \qquad (2.2)$$

where $U(t_f, t_i)$ is the time evolution operator in the interaction representation

$$U(t_f, t_i) = \mathrm{T} \exp\left[-i \int_{t_i}^{t_f} H_{\text{int},I}(t), dt\right]$$

$$= 1 - ie \int_{t_i}^{t_f} dt \int d^3 x J_I^\mu(\vec{x}, t) A_{\mu,I}(\vec{x}, t) + O(e^2), \qquad (2.3)$$

where the subscript I stands for the interaction representation in terms of H_0. In the above expression we have approximated $U(t_f, t_i)$ to first order in e, since we are interested in obtaining the probability of photon production to lowest order in the electromagnetic interaction. The usual S-matrix element for the transition is obtained from the transition amplitude $S(t_f, t_i)$ above in the limits $t_i \to -\infty$ and $t_f \to +\infty$

$$S_{fi} = S(+\infty, -\infty)$$

$$= -\frac{ie}{\sqrt{2E}} \int d^3 x \int_{-\infty}^{+\infty} dt\, e^{iP^\mu x_\mu} \varepsilon_\mu^\lambda \langle f|J^\mu(x)|i\rangle + O(e^2), \qquad (2.4)$$

where $E = |\vec{p}|$ and $P^\mu = (E, \vec{p})$ are the energy and four-momentum of the photon, respectively, and ε_μ^λ is its polarization four-vector. Since the states $|i\rangle$ and $|f\rangle$ are eigenstates of the *full* QCD Hamiltonian H_{QCD}, the above S-matrix element is obtained *to lowest order* in the electromagnetic interaction, but *to all orders* in the strong interaction. We note that the S-matrix element in effect is the amplitude for the transition between asymptotic states $|i; \text{in}\rangle \to |f, \gamma_\lambda(\vec{p}); \text{out}\rangle$, i.e., $S_{fi} = \langle f, \gamma_\lambda(\vec{p}); \text{out}|i; \text{in}\rangle$, where $|f, \gamma_\lambda(\vec{p}); \text{out}\rangle \equiv |f; \text{out}\rangle \otimes |\gamma_\lambda(\vec{p}); \text{out}\rangle$. Here, $|\gamma_\lambda(\vec{p}); \text{out}\rangle$ is the asymptotic *out* state with one photon of polarization λ and momentum $\vec{p}$, and $|i; \text{in}\rangle$ ($|f; \text{out}\rangle$) is the asymptotic *in* (*out*) state of the quarks and gluons.

The rate of photon production per unit volume from a QGP in thermal equilibrium at temperature T is obtained by squaring the S-matrix element, summing over the final states, and averaging over the initial states with the thermal weight $e^{-\beta E_i}/Z(\beta)$, where $\beta = 1/T$, E_i is the eigenvalue of H_0 corresponding to the eigenstate $|i\rangle$, and $Z(\beta) = \Sigma_i e^{-\beta E_i}$ is the partition function. Using the resolution of identity $1 = \Sigma_f |f\rangle\langle f|$, the sum of final states leads to the electromagnetic current correlation function. Upon using the transla-

tional invariance of this correlation function, the two space-time integrals lead to energy-momentum conservation multiplied by the space-time volume $\Omega = V(t_f - t_i)$ from the product of Dirac delta functions. The term $t_f - t_i \rightarrow +\infty$ is the usual interpretation of $2\pi\delta(0)$ in the square of the energy conserving delta functions.

These steps lead to the following result for the photon production rate in the S-matrix approach [2,6]:

$$\frac{dN}{d^4x} = \frac{1}{\Omega} \frac{1}{Z(\beta)} \frac{d^3p}{(2\pi)^3} \sum_{i,f,\lambda} e^{-\beta E_i} |S_{fi}|^2$$

$$= -e^2 g^{\mu\nu} W^{<}_{\mu\nu}(P) \frac{d^3p}{2E(2\pi)^3}, \qquad (2.5)$$

where $W^{<}_{\mu\nu}(K)$ is the Fourier transform of the thermal expectation value of the current correlation function defined by

$$W^{<}_{\mu\nu}(K) = \int d^4x \, e^{iK \cdot x} \langle J_\mu(0) J_\nu(x) \rangle_\beta. \qquad (2.6)$$

In the expression above $\langle \cdots \rangle_\beta$ denotes the thermal expectation value. To lowest order in e^2 but to all orders in the strong interactions, $W^{<}_{\mu\nu}(K)$ is related to the retarded photon self-energy $\Pi^R_{\mu\nu}(K)$ by [4]

$$e^2 W^{<}_{\mu\nu}(K) = \frac{\text{Im} \, \Pi^R_{\mu\nu}(\omega = k, k)}{e^{k/T} - 1}. \qquad (2.7)$$

Thus, one obtains the (Lorentz boost) invariant photon production rate

$$k\frac{dN}{d^3p \, d^4x} = -\frac{g^{\mu\nu}}{(2\pi)^3} \frac{\text{Im} \, \Pi^R_{\mu\nu}(\omega = k, k)}{e^{k/T} - 1}. \qquad (2.8)$$

All the calculations of the photon production yield from a thermalized QGP in equilibrium begin by obtaining $\text{Im} \, \Pi^R_{\mu\nu}(\omega = k, k)$ to calculate the *rate*. The most recent result up to leading logarithmic order in the strong coupling has been obtained in Ref. [8].

We have reproduced the steps leading to Eq. (2.8), which is the expression for the photon production rate used in all S-matrix calculations in the literature, to highlight several important steps in its derivation in order to compare and contrast to the real-time analysis discussed below. The main features of the above result that will be compared to the real time computation are the following:

(i) The initial states $|i\rangle$ are averaged with the thermal probability distribution at the initial time t_i for quarks and gluons. In the usual calculation this initial time $t_i \rightarrow -\infty$, as emphasized above and the initial state describes the photon vacuum and a thermal ensemble of quarks and gluons. Thus the quarks and gluons are assumed to have thermalized in the *infinite past*. Furthermore, this treatment also assumes that the quarks and gluons are *asymptotic* states in the infinite

past, thus neglecting the fact that these are confined in the colliding nuclei before the collision.

(ii) The transition amplitude is obtained via the time evolution operator $U(t_f, t_i)$ evolved up to a time t_f and the transition amplitude is obtained by projecting onto a state $|f\rangle$ at time t_f, which in the calculation is taken $t_f \rightarrow +\infty$. The sum over the final states leads to the electromagnetic current correlation function averaged over the initial states with the Boltzmann probability distribution, i.e., the thermal expectation value of the current correlation function.

(iii) Taking $t_f \rightarrow +\infty$ and $t_i \rightarrow -\infty$ and squaring the transition amplitude leads to *energy conservation* and an overall factor $t_f - t_i$. The rate (transition probability per unit time per unit volume V) is finally obtained by dividing by $(t_f - t_i)V$. The important point here is that taking the limit of $t_f - t_i \rightarrow +\infty$ results in *two* important aspects: energy conservation and an overall factor of the time interval $t_f - t_i$. The resulting rate is independent of the time interval and only depends on the photon energy (and obviously the temperature).

A. Main assumptions in the S-matrix approach

In order to compare our methods and results with those obtained within the usual S-matrix framework described above, it is important to highlight the main assumptions that are implicit in *all* previous calculations of photon production from a thermalized QGP and that are explicitly displayed by the derivation above.

(i) The initial state at t_i (which in the usual calculation is taken to $-\infty$) is taken to be a thermal equilibrium ensemble of quarks and gluons but the *vacuum state* for the physical transverse photons.

(ii) The usual calculation of the rate to lowest order in the electromagnetic coupling, entails that there are no electromagnetic corrections to the intermediate states, namely, there is no photon *dressing* of the states that enter in the thermal density matrix.

(iii) Taking $t_i \rightarrow -\infty, t_f \rightarrow +\infty$ manifestly assumes that quarks and gluons are *asymptotic states* in the infinite past and in the infinite future. Obviously this is inconsistent with the fact that before the collision quarks and gluons should be described in terms of their parton distribution functions in the nuclei. Furthermore assuming quarks and gluons to be asymptotic states as $t_f \rightarrow +\infty$ manifestly ignores the hadronization phase transition to a confined phase at a finite time of order 10–20 fm/c. In Ref. [9] confinement in the initial state had been encoded in a "confinement factor," namely a phenomenological parameter included to account for the effects of confinement.

(iv) Assuming the QGP to have equilibrated at $t_i \rightarrow -\infty$ and taking $t_f \rightarrow +\infty$ makes explicit that the plasma is assumed to be described as a stationary state in thermal equilibrium at all times.

(v) The buildup of population of photons is neglected along with the electromagnetic dressing of quarks, these assumptions are generally invoked to justify a calculation of the yield or rate to lowest order in the electromagnetic coupling.

(vi) The rate obtained from a stationary state of thermal equilibrium is then assumed to be valid in each fluid cell (of spatial size larger than the mean free path) which is taken as the local rest frame. The invariant rate (independent of time) is then written in terms of the proper time and fluid rapidity by performing a Lorentz boost and assuming that the temperature is a function of the proper time. The resulting rate is then integrated during the space-time history of the plasma in combination with a hydrodynamic description of the expansion. During the hadronization transition the yield is obtained from a Maxwell construction of the coexistence region (under the assumption of a first order transition). The lever rule is invoked to obtain the photon yield from the mixed phase. Thus despite the fact that the rate has been obtained by taking the initial and final times to $\mp\infty$ it is used to extract the photon yield during a *finite* lifetime, and even during phase coexistence [10–12].

B. Caveats

The main reason that we delve into the specific steps of the usual computation and the detailed analysis of the main assumptions is to emphasize the inconsistencies in applying this approach to an expanding QGP of *finite lifetime*.

(i) Hydrodynamic evolution is an *initial value problem* [21,22], namely, the state of the system is specified at an initial (proper) time surface to be of local thermodynamic equilibrium at a given initial temperature, and the hydrodynamic equations are evolved in time to either the hadronization or freeze-out surfaces if the equation of state is available for the different stages. The calculation based on the *S*-matrix approach takes the time interval to infinity, extracts a *time-independent rate* treating the QGP as a stationary state, and inputs this rate, assumed to be valid for every cell in the comoving fluid, in the hydrodynamic evolution during a finite lifetime.

(ii) There is also a physical inconsistency in using the *S*-matrix yield in a hydrodynamic evolution for very large photon energy. A hydrodynamic description, which is based on local thermodynamic equilibrium, is valid on spatial scales larger than the mean free path for parton-parton collisions in the plasma $\lambda \sim 0.5$ fm. Thus photon momenta $k \geqslant 2-3$ GeV probe distances shorter than the mean free path, and most likely the contribution to the direct photon spectrum for transverse momenta larger than about 2–3 GeV cannot be reliably extracted from an *S*-matrix calculation. Recent measurements of elliptic flow at RHIC [14] suggest that hydrodynamics is a reliable description up to $p_T \sim 2$ GeV/c but the data for $v_2(p_T)$ show large departures from hydrodynamics (including pQCD) for $p_T > 2$ GeV/c for charged particles (minimum bias) [23].

The low energy region of the photon spectrum is dominated by pion decay and bremsstrahlung in the hadronic phase and after freeze-out. Thus, the (transverse) momentum interval in which direct photons could be reliable experimental probes of a thermalized QGP is 0.1 GeV $\lesssim k \lesssim 3$ GeV.

(iii) Yet another caveat is that despite the fact that the time interval is taken to infinity, namely much larger than the photon thermalization time scale, photons are assumed *not to*

thermalize and to leave the medium. The buildup of the photon population is *neglected* under the assumption that the mean free path of the photons is larger than the size of the plasma and the photons escape without rescattering. This assumption also neglects the prompt photons produced during the preequilibrium stage. Indeed, Srivastava and Geiger [24] have studied direct photons from a preequilibrium stage via a parton cascade model that includes pQCD parton cross sections and electromagnetic branching processes. The usual computation of the prompt photon yield during the stage of a *thermalized* QGP assumes that these photons have left the system and the computation is therefore carried out to lowest order in α_{em} with an initial photon vacuum state, namely also ignoring the virtual cloud of photons that dress the charged particles in the plasma. As emphasized above, in taking the final time t_f to infinity in the *S*-matrix element the assumption is that the thermalized state is *stationary*, while in neglecting the buildup of the population the assumption is that the photons leave the system without rescattering and the photon population never builds up. These assumptions lead to considering photon production only to the lowest order in α_{em}, since the buildup of the photon population will necessarily imply higher order corrections. Although these main assumptions are seldom spelled out in detail, they underlie all *S*-matrix calculations of the photon production from a thermalized QGP.

All calculations of the rate based on the *S*-matrix approach, obtain the imaginary part of the photon polarization to lowest order in α_{em} and in a perturbative expansion in terms of α_s (including leading logarithmic terms). This expansion assumes that α_s is small but the coupling depends on the temperature scale. While it could be argued that at the initial temperatures expected to be achieved at RHIC and LHC α_s may be small, clearly the perturbative expansion breaks down in the expanding scenario, when the temperature becomes near the critical for hadronization $T_c \sim \Lambda_{QCD} \sim 160$ MeV. Thus, the regime of validity of *all S*-matrix calculations of the yield in a perturbative expansion in α_s is actually limited by the *lifetime* of the QGP. Hence a perturbative evaluation of the rate must be understood to be valid on a time scale of the order of or shorter than the actual lifetime of the QGP, which then casts further doubts on the infinite time limit.

As stated in the Introduction, however, the QGP produced in ultrarelativistic heavy ion collisions is intrinsically a transient and nonequilibrium state. Since the spectrum of direct photons is deemed to be a clean experimental probe of the early stages of evolution of a QGP, it is therefore of phenomenological importance to study nonequilibrium effects on direct photon production from an expanding QGP with a *finite lifetime* with the goal of establishing potential experimental signatures.

The current understanding of the QGP formation, equilibration, and subsequent evolution through the quark-hadron (and chiral) phase transitions is summarized as follows. A preequilibrium stage dominated by parton-parton interactions and strong colored fields which gives rise to quark and gluon production on time scales $\lesssim 1$ fm/c [15]. The produced quarks and gluons thermalize via elastic collisions on time

scales ~ 1 fm/c. Hydrodynamics is probably the most frequently used model to describe the evolution of the next stage when quarks and gluons are in local thermal equilibrium (although perhaps not in chemical equilibrium) [21,22]. The hydrodynamical picture assumes local thermal equilibrium (LTE), a fluid form of the energy-momentum tensor and the existence of an equation of state for the QGP. The subsequent evolution of the QGP is uniquely determined by the hydrodynamical equations, which are formulated as an *initial value problem* with the initial conditions specified at the moment when the QGP reaches LTE, i.e., at an initial time t_i ~ 1 fm/c. The (adiabatic) expansion and cooling of the QGP is then followed to the transition temperature at which the equation of state is matched to that describing the mixed and hadronic phases [6,10,25,26].

Our main observation is that the usual computations based on S-matrix theory extract a time independent rate after taking the infinite time interval, which is then used in a calculation of the photon yield during a *finite time* hydrodynamic evolution. There is a conceptual inconsistency in this approach, which merits a detailed study based on the real time evolution of the photon distribution, which we undertake below.

III. REAL TIME APPROACH

A. Gauge invariance

Before we focus on the calculation of the photon yield in real time, we address the issue of Abelian gauge invariance to highlight that the results of the real time approach are fully gauge invariant. Since the relevant interaction is electromagnetic, we focus our discussion on the Abelian gauge coupling. Let us consider the following Lagrangian density for one massless fermion species:

$$\mathcal{L}=\bar{\psi}(i\slashed{\partial}-e\slashed{A})\psi-\frac{1}{4}F_{\mu\nu}F^{\mu\nu}, \qquad (3.1)$$

where the zero-temperature mass of the fermion m has been neglected since we consider the high temperature limit T $\gg m$. We begin by casting our study directly in a manifestly gauge invariant form. In the Abelian case it is straightforward to reduce the Hilbert space to the gauge invariant states and to define gauge invariant fields. This is best achieved within the canonical Hamiltonian formulation in terms of primary and secondary class constraints. In the Abelian case there are two first class constraints:

$$\pi_0=0, \quad \boldsymbol{\nabla}\cdot\boldsymbol{\pi}=-e\,\psi^\dagger\psi, \qquad (3.2)$$

where π_0 and $\boldsymbol{\pi}=-\mathbf{E}$ are the canonical momenta conjugate to A^0 and $\mathbf{A}$, respectively. Physical states are those which are simultaneously annihilated by the first class constraints and physical operators *commute* with the first class constraints. Writing the gauge field in terms of transverse and longitudinal components as $\mathbf{A}=\mathbf{A}_L+\mathbf{A}_T$ with $\boldsymbol{\nabla}\times\mathbf{A}_L=0$; $\boldsymbol{\nabla}\cdot\mathbf{A}_T=0$ and defining

$$\Psi(x)=\psi(x)e^{ie\int d^3y\,\boldsymbol{\nabla}_\mathbf{x}G(\mathbf{x}-\mathbf{y})\cdot\mathbf{A}_L(y)}, \qquad (3.3)$$

where $G(\mathbf{x}-\mathbf{y})$ is the Coulomb Green's function satisfying $\boldsymbol{\nabla}_\mathbf{x}^2G(\mathbf{x}-\mathbf{y})=\delta^3(\mathbf{x}-\mathbf{y})$, after some algebra using the canonical commutation relations one finds that $\mathbf{A}_T(x)$ and $\Psi(x)$ are *gauge invariant* field operators.

The Hamiltonian can now be written solely in terms of these gauge invariant operators and when acting on gauge invariant states the resulting Hamiltonian is equivalent to that obtained in a Coulomb gauge. However we emphasize that we have *not* fixed any gauge; this treatment, originally introduced by Dirac, is manifestly gauge invariant. The instantaneous Coulomb interaction can be traded for a gauge invariant Lagrange multiplier field which we call A^0, leading to the following Lagrangian density:

$$\mathcal{L}=\bar{\Psi}(i\slashed{\partial}-e\,\gamma^0A^0+e\,\boldsymbol{\gamma}\cdot\mathbf{A}_T)\Psi$$
$$+\frac{1}{2}[(\partial_\mu\mathbf{A}_T)^2+(\boldsymbol{\nabla}A^0)^2]. \qquad (3.4)$$

We emphasize that A^0 should *not* be confused with the temporal gauge field component.

In the gauge invariant sector of the Hilbert space, namely between states annihilated by the first class constraints, and generalizing to N_f flavors of quarks, the Hamiltonian is given by

$$H=\int d^3x\left[\frac{1}{2}(\vec{E}_T^2+\vec{B}^2)+\Psi^\dagger\right.$$
$$\left.\times(-i\vec{\alpha}\cdot\vec{\nabla})\Psi+e\vec{J}\cdot\vec{A}_T\right]+H_{Coul}, \qquad (3.5)$$

where

$$\vec{J}=\sum_{i=1}^{N_f}\frac{e_i}{e}\bar{\Psi}_i\vec{\gamma}\Psi_i, \qquad (3.6)$$

is the *gauge* invariant current and H_{Coul} is the Abelian Coulomb interaction which will be irrelevant for our considerations. While this Hamiltonian is equivalent to that obtained in a Coulomb gauge we emphasize that we have not imposed any gauge fixing; the Dirac procedure is manifestly gauge invariant. In particular the interaction part of the Hamiltonian that will be relevant for the discussion of photon production to lowest order, namely

$$H_I=e\int d^3x\vec{J}\cdot\vec{A}_T \qquad (3.7)$$

is manifestly gauge invariant. Furthermore, states constructed out of the noninteracting Fock vacuum by combinations of the *gauge invariant* operators $\Psi^\dagger,\Psi,\vec{A}_T,\vec{E}_T$ are obviously gauge invariant.

This discussion makes explicit the gauge invariance of the real time formulation.

Including now the non-Abelian color interaction between quarks and gluons the total Hamiltonian is given by

$$H = H_{QCD}[\Psi] + \int d^3x \frac{1}{2}(\vec{E}_T^2 + \vec{B}^2)$$

$$+ e \int d^3x \mathbf{J} \cdot \mathbf{A}_T + H_{Coul},\tag{3.8}$$

where $H_{QCD}[\Psi]$ is the QCD Hamiltonian in absence of electromagnetism but in terms of the gauge invariant (under Abelian gauge transformation) fermion field Ψ and the subscript T refers to transverse components. We have extended the fermion content to N_f flavors and the charge of each flavor species in units of the electron charge is included in the corresponding current.

Expanding the gauge invariant field $\vec{A}_T$ in terms of creation and annihilation operators in a volume V

$$\mathbf{A}_T(\vec{x}) = \sum_{\mathbf{k},\lambda} \frac{\boldsymbol{\epsilon}_{\mathbf{k},\lambda}}{\sqrt{2Vk}}[a_{\mathbf{k},\lambda}e^{i\mathbf{k}\cdot\mathbf{x}} + a_{\mathbf{k},\lambda}^\dagger e^{-i\mathbf{k}\cdot\mathbf{x}}],\tag{3.9}$$

with $\boldsymbol{\epsilon}_{\mathbf{k},\lambda}$ the usual transverse polarization vectors, the *gauge invariant* photon number operator for polarization λ is given by

$$\hat{n}_{\mathbf{k},\lambda} = a_{\mathbf{k},\lambda}^\dagger a_{\mathbf{k},\lambda}.\tag{3.10}$$

B. Time evolution

Time evolution in quantum mechanics and quantum field theory is an initial value problem. Given the total Hamiltonian H the time evolution of a density matrix is completely determined by specifying the density matrix at an initial time t_0. Once the initial density matrix is specified at the initial time, its time evolution is completely determined by the unitary time evolution operator $e^{-iH(t-t_0)}$. In the case under consideration the Hamiltonian H is *time independent and gauge invariant* and given by Eq. (3.8). The ensuing real time dynamics is therefore completely specified by prescribing the initial density matrix at the initial time t_0.

As discussed above, the S-matrix calculation implicitly assumes that the initial density matrix is that of thermal equilibrium for quarks and gluons at an initial time $t_0 = -\infty$ and explicitly assumes that initially there are no photons. With this choice of initial conditions, since the initial state has been prepared at $t_0 = -\infty$ there is no memory of the initial state, in agreement with a stationary state in thermodynamic equilibrium.

Our goal is to relax this assumption of a thermal stationary state and study the consequences of a true real time evolution as befits the physical problem of a thermalized QGP emerging about 1 fm/c after a nucleus-nucleus collision and evolving during a finite lifetime of about 10–20 fm/c towards a hadronization (and confinement) transition.

The real time evolution of the density matrix after the initial time t_0 is given by

$$\hat{\rho}(t) = e^{-iH(t-t_0)}\hat{\rho}(t_0)e^{iH(t-t_0)}.\tag{3.11}$$

The total number of photons of momentum k per unit volume at a given time t, namely the photon yield is given by (assuming translational invariance)

$$(2\pi)^3 \frac{dN(t)}{d^3x d^3k} = \sum_\lambda \text{Tr}[\hat{\rho}(t)\hat{n}_{\mathbf{k},\lambda}],\tag{3.12}$$

with $\hat{n}_{\mathbf{k},\lambda} = \hat{a}_{\mathbf{k},\lambda}^\dagger \hat{a}_{\mathbf{k},\lambda}$. In order to compute the direct photon yield to lowest order in the electromagnetic coupling, it is convenient to write the total Hamiltonian given by Eq. (3.8) as

$$H = H_0 + H_I,$$

$$H_0 = H_{QCD}[\Psi] + \int d^3x \frac{1}{2}(\vec{E}_T^2 + \vec{B}^2),$$

$$H_I = \int d^3x \mathbf{J} \cdot \mathbf{A}_T,\tag{3.13}$$

where the current $\mathbf{J}$ is given by Eq. (3.6) and we have neglected the Coulomb term since it will not contribute to the direct photon yield to order α_{em}.

The time evolution operator is given by

$$e^{-iH(t-t_0)} = e^{-iH_0 t}U(t,t_0)e^{iH_0 t_0},\tag{3.14}$$

where $U(t,t_0)$ is the unitary time evolution operator in the interaction picture of H_0 given by

$$U(t,t_0) = 1 - i\int_{t_0}^t dt' H_I(t') + O(e^2);$$

$$H_I(t) = e^{iH_0 t}H_I e^{-iH_0 t},\tag{3.15}$$

where we have only considered the lowest order in the electromagnetic coupling.

It is then convenient to pass to the interaction picture of H_0, namely the full QCD Hamiltonian and *free* electromagnetism by defining the initial density matrix in the interaction picture of H_0 as

$$\hat{\rho}_{ip}(t_0) = e^{iH_0 t_0}\hat{\rho}(t_0)e^{-iH_0 t_0}.\tag{3.16}$$

For the case of interest the initial density matrix describes a quark gluon plasma in equilibrium under the strong interac-

tions, it must therefore commute with H_0 in which case $\hat{\rho}_{ip}(t_0) = \hat{\rho}(t_0)$. At any given time t

$$\hat{\rho}(t) = e^{-iH_0 t} U(t,t_0) \hat{\rho}_{ip}(t_0) U^{-1}(t,t_0) e^{iH_0 t}. \quad (3.17)$$

Since the number operator $a_{\mathbf{k},\lambda}^\dagger a_{\mathbf{k},\lambda}$ commutes with H_0 we find for the direct photon yield at time t the following exact expression:

$$(2\pi)^3 \frac{dN(t)}{d^3 x d^3 k} = \sum_\lambda \text{Tr}[U(t,t_0) \hat{\rho}_{ip}(t_0) U^{-1}(t,t_0) \hat{n}_{\mathbf{k},\lambda}]. \quad (3.18)$$

In the interaction picture of H_0 the time evolution of $\mathbf{J}$ and $\mathbf{A}_T$ is given by

$$\mathbf{J}(\vec{x},t') = e^{iH_{QCD}t'} \mathbf{J}(\vec{x}) e^{-iH_{QCD}t'},$$

$$\mathbf{A}_T(\vec{x},t') \sum_{\mathbf{k},\lambda} \frac{\boldsymbol{\epsilon}_{\mathbf{k},\lambda}}{\sqrt{2Vk}} [a_{\mathbf{k},\lambda} e^{i\mathbf{k}\cdot\mathbf{x}} e^{-ikt'} + a_{\mathbf{k},\lambda}^\dagger e^{-i\mathbf{k}\cdot\mathbf{x}} e^{ikt'}], \quad (3.19)$$

where $\boldsymbol{\epsilon}_{\mathbf{k},\lambda}$ are the transverse polarization vectors.

Given an initial density matrix, the photon yield can be calculated by inserting a complete set of eigenstates of H_0 and computing the required matrix elements.

We note that the real time expression for the photon yield Eq. (3.18) is *exact* in terms of the full time independent Hamiltonian and is gauge invariant provided that the density matrix is constructed with physical states. Evolution of quantum states or density matrices is an initial value problem, once the density matrix has been specified at an initial time, its time evolution is completely determined by the Hamiltonian.

We carry out this program below to lowest order in the electromagnetic coupling for cases that are relevant to the description of direct photons from a QGP.

IV. PHOTON YIELD

We compute here the photon yield for a QGP with finite lifetime in the real time approach.

A. Thermalized QGP, no initial photons

We begin the study of the real time dynamics of direct photon production by considering that at an initial time t_0 ~ 1 fm/c the QGP is in thermal equilibrium (under the

strong interactions) and there are *no initial photons*. Such an initial density matrix is compatible with the usual assumption on the initial state invoked in the S-matrix calculation described in Sec. II but makes explicit that such a state describes an initial value problem from a thermalization time t_0 taken to be of the order of 1 fm/c,

$$\hat{\rho}(t_0) = \sum_{n_q} e^{-\beta E_{n_q}} |n_q\rangle\langle n_q| \otimes |0_\gamma\rangle\langle 0_\gamma|;$$

$$H_{QCD}|n_q\rangle = E_{n_q}|n_q\rangle, \quad (4.1)$$

and $|0_\gamma\rangle$ is the photon vacuum, annihilated by the *gauge invariant operators* $a_{\mathbf{k},\lambda}$. The incoming nuclei coasting along the light cone are exact eigenstates of the full Hamiltonian H. Hence, neglecting bremsstrahlung off the Coulomb field of the nuclei there is no photon emission prior to the collision. Thus, the state $|0_\gamma\rangle$ is the "in" state up to the time of the collision, which is annihilated by the "in" operator $a_{\mathbf{k},\lambda}$. Therefore the initial density matrix Eq. (4.1) is consistent with neglecting the photons produced between the collision and the onset of thermalization, namely during the preequilibrium stage.

We will study in detail alternative and more general initial states that include photons and correlations in a later section (see Sec. V below).

Obviously the initial density matrix given by Eq. (4.1) is gauge invariant and commutes with H_0 in Eq. (3.14). It follows that $\hat{\rho}(t_0) = \hat{\rho}_{ip}(t_0)$ and it describes a thermal ensemble in equilibrium under the strong interactions with no photons. This assumption is compatible with *all the calculations* of direct photon production from an equilibrated QGP available in the literature. Studying the time evolution of this initial state allows us to address the dynamics of the formation of the virtual photon cloud and to highlight the inherent difficulty in separating the observable photons from those in the virtual cloud in the plasma during a finite lifetime.

Defining as $|n_q; m_\gamma\rangle = |n_q\rangle \otimes |m_\gamma\rangle$ the eigenstates of H_0 with m_γ photons (we do not specify the wave vector and polarization to avoid cluttering of notation) we can compute the matrix elements in Eq. (3.18) by inserting a complete set of these eigenstates. To lowest order in the electromagnetic coupling the set of intermediate states that contribute to the photon number $\langle \hat{n}_{\mathbf{k},\lambda} \rangle$ contain only one photon of momentum k and polarization λ.

After a straightforward calculation we find, to lowest order in the electromagnetic coupling

$$(2\pi)^3 \frac{dN(t)}{d^3 x d^3 k} = \sum_\lambda \frac{e^2}{2kV} \int_{t_0}^t dt_1 \int_{t_0}^t dt_2 \int d^3 x_1 \int d^3 x_2 e^{-ik(t_2-t_1)} e^{i\mathbf{k}\cdot(\mathbf{x}_2-\mathbf{x}_1)}$$

$$\times \sum_{n_q,m_q} e^{-\beta E_{n_q}} \langle n_q|\boldsymbol{\epsilon}_{\mathbf{k},\lambda}\cdot\mathbf{J}(\vec{x_2},t_2)|m_q\rangle\langle m_q|\boldsymbol{\epsilon}_{\mathbf{k},\lambda}\cdot\mathbf{J}(\vec{x_1},t_1)|n_q\rangle. \quad (4.2)$$

Writing,

$$\mathbf{J}(\vec{x},t) = e^{-i\vec{P}\cdot\vec{x}} e^{iH_{QCD}t} \mathbf{J}(\vec{0},0) e^{-iH_{QCD}t} e^{i\vec{P}\cdot\vec{x}}, \quad (4.3)$$

with $\vec{P}$ the momentum operator and choosing the eigenstates $|n_q\rangle$ to be simultaneous eigenstates of $\vec{P}$ with $\vec{P}|n_q\rangle = \vec{p}_{n_q}|n_q\rangle$, we can write

$$\sum_{n_q,m_q} e^{-\beta E_{n_q}} \langle n_q | \boldsymbol{\epsilon}_{\mathbf{k},\lambda} \cdot \mathbf{J}(\vec{x_2},t_2) | m_q \rangle \langle m_q | \boldsymbol{\epsilon}_{\mathbf{k},\lambda} \cdot \mathbf{J}(\vec{x_1},t_1) | n_q \rangle$$

$$= \int d^3p \, d\omega \, e^{-i\vec{p}\cdot(\vec{x_2}-\vec{x_1})} e^{i\omega(t_2-t_1)} \epsilon^i_{\mathbf{k},\lambda} \epsilon^j_{\mathbf{k},\lambda} \sigma^>_{ij}(\vec{p},\omega), \quad (4.4)$$

where

$$\sigma^>_{ij}(\vec{p},\omega) = \sum_{n_q,m_q} e^{-\beta E_{n_q}} \langle n_q | J_i(\vec{0},0) | m_q \rangle \langle m_q | J_j(\vec{0},0) | n_q \rangle$$

$$\times \delta^3(\vec{p} - (\vec{p}_{n_q} - \vec{p}_{m_q})) \delta(\omega - (E_{n_q} - E_{m_q})). \quad (4.5)$$

Carrying out the integrals in Eq. (4.2) and summing over the polarizations, we finally find,

$$\frac{dN(t)}{d^3x \, d^3k}$$

$$= \frac{e^2}{k} \int d\omega \, \mathcal{P}^{ij}(\mathbf{k}) \sigma^>_{ij}(\vec{k},\omega) \frac{1-\cos[(\omega-k)(t-t_0)]}{(\omega-k)^2}, \quad (4.6)$$

where

$$\mathcal{P}^{ij}(\mathbf{k}) = \delta^{ij} - \frac{k^i k^j}{k^2}, \quad (4.7)$$

is the transverse projector.

In the Appendix we show that

$$(2\pi)^3 e^2 \sigma^>_{ij}(\vec{k},\omega) = \frac{n(\omega)}{\pi} \operatorname{Im} \Pi_{ij}(\vec{k},\omega); $$

$$n(\omega) = \frac{1}{e^{\beta\omega}-1}, \quad (4.8)$$

where $\operatorname{Im} \Pi_{ij}(\vec{k},\omega)$ is the imaginary part of the retarded photon polarization tensor. However, the photon production yield is calculated to lowest order in α_{em} and in principle to all orders in α_s.

Introducing the transverse photon polarization

$$\Pi_T(k,\omega) \equiv \mathcal{P}^{ij}(\mathbf{k}) \Pi_{ij}(\vec{k},\omega), \quad (4.9)$$

we finally find the real time expression for the photon yield to be given by

$$\frac{dN(t)}{d^3x \, d^3k}$$

$$= \frac{1}{(2\pi)^3 k} \int_{-\infty}^{+\infty} \frac{d\omega}{\pi} \frac{\operatorname{Im} \Pi_T(k,\omega)}{e^{\omega/T}-1} \frac{1-\cos[(\omega-k)(t-t_0)]}{(\omega-k)^2}, \quad (4.10)$$

where the photon polarization is obtained in lowest order in α_{em} and in principle to all orders in α_s. This expression coincides with the lowest order result obtained from a kinetic description in Ref. [20].

If the long time limit is taken and the following identity is used (see [20,27]):

$$\int_{-\infty}^{+\infty} d\omega F(\omega) \frac{1-\cos[(\omega-k)(t-t_0)]}{(\omega-k)^2}$$

$$\stackrel{t-t_0 \to +\infty}{\times} = \pi(t-t_0)F(k) + \int_{-\infty}^{+\infty} d\omega F(\omega) \mathcal{P} \frac{1}{(\omega-k)^2}$$

$$+ O\left(\frac{1}{t-t_0}\right), \quad (4.11)$$

then *if* $\operatorname{Im} \Pi_T(k,\omega=k) \neq 0$, we obtain the long time limit of the total yield,

$$\frac{dN(t)}{d^3x \, d^3k} = \frac{1}{(2\pi)^3 k} \left\{ \frac{\operatorname{Im} \Pi_T(k,\omega=k)}{e^{k/T}-1} (t-t_0) \right.$$

$$\left. + \int_{-\infty}^{+\infty} \frac{d\omega}{\pi} \frac{\operatorname{Im} \Pi_T(k,\omega)}{e^{\omega/T}-1} \mathcal{P} \frac{1}{(\omega-k)^2} \right\}. \quad (4.12)$$

From the result (4.12) above, we obtain the long time limit of the invariant rate,

$$k \frac{dN(t)}{d^4x \, d^3k} \stackrel{t-t_0 \to +\infty}{=} \frac{1}{(2\pi)^3} \frac{\operatorname{Im} \Pi_T(k,\omega=k)}{e^{k/T}-1}. \quad (4.13)$$

This is the same as the *S*-matrix result given by Eq. (2.8).

The expression (4.12) only involves the *transverse* part of the photon polarization, a consequence of the manifestly gauge invariant treatment. Thus, we highlight that in the *infinite time limit* our result for the invariant rate coincides with the usual one.

However, taking the time to infinity introduces all the caveats that were discussed in Sec. II above. Thus, in order to avoid these caveats, the initial time t_0 must be interpreted as the time at which quarks and gluons thermalize. The expression (4.10) determines the total photon yield (per unit volume) at a given time t, thus the total direct photon yield at the hadronization time is obtained by setting $t = t_{had} \sim 10$–20 fm/c for RHIC and LHC respectively.

The asymptotic long time expression (4.12), features *two* different terms. The first term, which grows linearly in time leads to the *rate* which is time independent and is associated with the photons that are produced per unit time per unit volume. The second, time independent term can be interpreted as the total number of photons in the virtual cloud dressing the quarks in the medium.

This manifest separation between the time independent term that describes the photon cloud associated with the charged particles, and the photons produced at constant rate (namely the term in the yield that grows linearly with $t - t_0$) *only emerges* in the long time limit.

For any *finite* time interval there are contributions to the photon yield from the whole range of $\omega \neq k$. The long time asymptotic behavior of the total photon yield (4.10) is determined by the behavior of $\text{Im}\,\Pi(\omega \sim k)$. In particular if $\text{Im}\,\Pi(k, \omega = k) = 0$ there is no *linear* time dependence asymptotically, however if $\text{Im}\,\Pi(\omega \sim k) \propto (\omega - k)$ as is the case for the one loop contribution to the polarization [of $O(\alpha_{em}\alpha_s)$, see below] then using the formula [20,27]

$$\int_0^{+\infty} dy\, \frac{p(y)}{y}[1 - \cos(ykt)] \overset{t \to +\infty}{=} p(0)\ln(kt) + O(1),$$

(4.14)

for $p(\infty) = 0$. We thus conclude that the photon yield will grow *logarithmically in time* in this case.

The long time behavior of the yield is therefore determined by the behavior of the $\text{Im}\,\Pi(k, \omega)$ in the region $\omega \sim k$. Generally, the imaginary part of the photon polarization for $\omega \sim k$ behaves as

$$\text{Im}\,\Pi_T(k, \omega) \overset{\omega \to k}{=} \text{Im}\,\Pi_T(k, \omega = k) + \text{Im}\,\Pi'_T(k, \omega = k)(\omega - k)$$
$$+ O[(\omega - k)^2],$$

(4.15)

then we find [20,27] the long time behavior of the yield to be generally given by

$$\frac{dN(t)}{d^3x\, d^3k} = \frac{1}{(2\pi)^3 k}\left\{\frac{\text{Im}\,\Pi_T(k, \omega = k)}{e^{k/T} - 1}(t - t_0)\right.$$
$$+ \frac{\text{Im}\,\Pi'_T(k, \omega = k)}{\pi(e^{k/T} - 1)}\ln[k(t - t_0)]$$
$$\left. + \int \frac{d\omega}{\pi}\, \frac{\text{Im}\,\Pi_T(k, \omega)}{e^{\omega/T} - 1}\mathcal{P}\frac{1}{(\omega - k)^2} + O\left(\frac{1}{t - t_0}\right)\right\},$$

(4.16)

where the prime in the second term stands for a derivative with respect to the frequency. Obviously at very long times the term with the linear time dependence will ultimately dominate. However, for a finite time interval $(t - t_0)$, it is possible that a lower order logarithmic term may give a comparable contribution to or even be larger than a higher order term linear in time. Furthermore, it is clear from the above analysis that the contributions to the imaginary part of the photon polarization for $\omega \neq k$ will actually contribute to the yield during a finite time interval. However, these contributions are absent in the *S*-matrix calculation which only extracts the linear time dependence in the *asymptotic long time limit* given by Eq. (4.13).

The main point of this discussion is to highlight the following important issues:

(i) The real time calculation reproduces the result of the *S*-matrix approach in the asymptotic long time limit. Therefore the usual *S*-matrix result is *contained* in the real time approach, which provides a detailed description of the process of photon production during a finite lifetime.

(ii) During a finite time interval the region $\omega \neq k$ of the imaginary part of the photon polarization contributes. The contributions from different regions of the spectral density have different time dependence. During a finite time interval contributions that are subleading in the asymptotic long time limit can be of the same order as the term that becomes asymptotically linear in time and which defines the rate. In a finite time interval the contributions from the different regions in the frequency integral cannot be separated. Thus, in order to reliably understand the time dependence of the yield during a finite time interval, one must find the imaginary part of the photon polarization in the *full range* of frequency, not just at $\omega = k$ which only determines the asymptotic long time behavior.

(iii) This discussion makes manifestly clear that the photon *yield* obtained from the *S*-matrix calculation of the rate, namely extracting the linear time dependence in the asymptotic long time limit, ignores all other contributions which grow slower in time but that do contribute to the yield for a finite time interval.

B. Photon production in the hard thermal loop approximation

To make the above statement more quantitative and to begin our study of the real time description of photon production within a specific example highlighting the conclusions above, we begin by considering the imaginary part of the photon polarization tensor in the hard thermal loop ap-

proximation [28,29]. This approximation yields the leading result for the polarization tensor for soft photons, namely $k \ll T$ and arises *solely* from in-medium processes. While we will obtain the full one-loop contribution to the imaginary part of the photon self-energy below, the HTL limit *only* features medium dependent contributions. Thus the HTL limit allows us to address dynamical issues solely associated with in-medium processes.

For two flavor of quarks (up and down, with three colors), the imaginary part of the transverse photon polarization in the hard thermal loop approximation is given by [20]

$$\operatorname{Im}\Pi_T^{HTL}(k,\omega) = \frac{40\pi^2\alpha_{em}T^2}{36}\frac{\omega}{k}\left(1 - \frac{\omega^2}{k^2}\right)\Theta(k^2 - \omega^2).$$

$$(4.17)$$

Obviously this contribution to the imaginary part vanishes linearly as $\omega \to k$. However, while Eq. (4.12) would lead to a constant, time independent yield and therefore to a vanishing invariant rate since $\operatorname{Im}\Pi_{ij}(\omega=k)=0$, the correct asymptotic long time limit of the yield follows from Eq. (4.16) and is given by [20]

$$\frac{dN^{HTL}(t)}{d^3xd^3k}\Bigg|^{t-t_0 \to +\infty} = \frac{5\alpha_{em}T^2}{18\pi^2k^2}\Bigg[n(k)\ln[k(t-t_0)]$$

$$+ \frac{1}{2k}\int_{-k}^{k}d\omega\frac{\omega}{k}\mathcal{P}\left[\frac{k+\omega}{k-\omega}\right]\frac{1}{e^{\omega/T}-1}$$

$$+ O\left(\frac{1}{t-t_0}\right)\Bigg].$$

$$(4.18)$$

This expression would lead to an invariant rate that vanishes as $O(1/t)$ for $t \to +\infty$. However, for any finite time there is a nonvanishing contribution to the yield.

The second, time independent term in Eq. (4.18) can be identified with the virtual photon cloud *in the thermal bath*. This contribution is medium dependent and can only be identified in the long time limit; the separation between the time independent and the time dependent contributions is meaningful only in the long time limit. For any finite lifetime there is no unambiguous separation between the different contributions, and only the full photon number is meaningful.

A comparison with the photon equilibrium spectral density in the HTL approximation [29] reveals that the integrand of the time independent part in Eq. (4.18) is simply related to the HTL wave function renormalization and the real part of the photon polarization. Namely, the virtual cloud is actually revealing the dynamics of formation of a plasmon quasiparticle in the medium.

The result Eq. (4.18) is valid in the asymptotic long time limit; for any arbitrary finite time we must use the full expression given by Eq. (4.10). In particular, in the hard thermal loop limit we find that the yield is given by
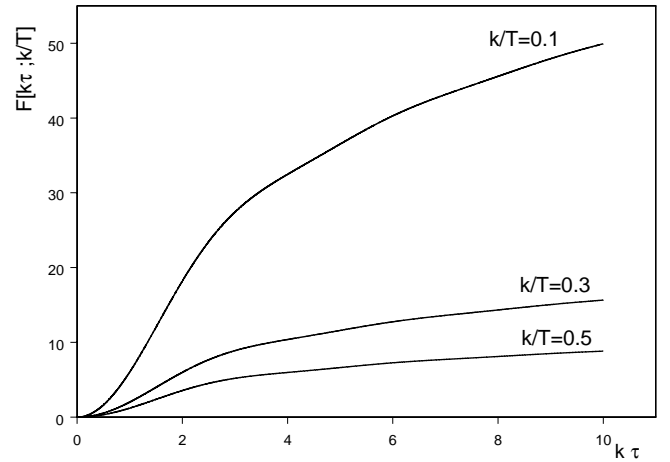

FIG. 1. The function $\mathcal{F}[k\tau;k/T]$ vs $k\tau$ for $k/T = 0.1;0.3;0.5$ respectively.

$$\frac{dN^{HTL}(t)}{d^3xd^3k} = \frac{5}{36\pi^2}\frac{\alpha_{em}T^2}{k^2}\mathcal{F}\left[k(t-t_0);\frac{k}{T}\right],$$

$$\mathcal{F}\left[k\tau;\frac{k}{T}\right] = \int_{-1}^{1}dxn\left[x\frac{k}{T}\right]x(1-x^2)$$

$$\times\frac{1-\cos[(x-1)k\tau]}{(x-1)^2}.$$

$$(4.19)$$

The function $\mathcal{F}[k\tau;k/T]$ is displayed in Fig. 1 for several values of the ratio k/T. This figure displays the logarithmic growth determined by the asymptotic behavior (4.18) at long times.

C. Full one loop polarization

As mentioned in the Introduction, we will study the dynamics of photon production during a finite lifetime by focusing on the lowest order contribution to the photon polarization. This is a quark one loop diagram and is of order α_{em}. The imaginary part of this diagram vanishes at $\omega=k$, hence this lowest order diagram does not contribute to the usual rate obtained from the long time limit as discussed in detail above.

The goal of this study is to understand the photon production during the finite lifetime of the QGP from processes whose contribution is subleading in the asymptotic long-time limit. Of course diagrams which are higher order in α_s will also give contributions to the photon production from the region $\omega \neq k$, but focusing on the lowest order diagram we will be able to extract important aspects of the dynamics that are missed by the S-matrix calculation and that could be experimentally relevant.

A comparison between real time yield obtained from the one loop contribution to the photon polarization and the S-matrix yield in a wide range of photon energy, in particular for large photon momentum, requires the full expression for the photon polarization to one loop order.

A lengthy but straightforward calculation gives the following result:

$$\text{Im}\,\Pi^T(\omega,k) = \pi_0(\omega,k) + \pi_{LD}(\omega,k) + \pi_{2P}(\omega,k)$$
(4.20)

with $\pi_0; \pi_{2P}$ and π_{LD} the zero temperature, two fermion thermal cut and Landau damping contributions, respectively, given by the following expressions:

$$\pi_0(\omega,k) = \frac{10}{9}\alpha_{em}(\omega^2-k^2)\Theta(\omega^2-k^2)\text{sgn}(\omega),$$
(4.21)

$$\pi_{2P}(\omega,k) = \frac{10}{3}\alpha_{em}T^2\left(\frac{\omega^2}{k^2}-1\right)\left[\frac{k}{T}\ln\left(\frac{1+e^{-W_+}}{1+e^{-W_-}}\right)\right.$$
$$-\frac{2T}{k}\sum_{m=1}^{\infty}(-1)^{m+1}\left[\frac{2}{m^3}(e^{-mW_-}-e^{-mW_+})\right.$$
$$\left.-\frac{k}{Tm^2}(e^{-mW_-}+e^{-mW_+})\right]\Theta(\omega^2-k^2)\text{sgn}(\omega),$$
(4.22)

$$\pi_{LD}(\omega,k) = \frac{10}{3}\alpha_{em}T^2\left(1-\frac{\omega^2}{k^2}\right)\left[\frac{k}{T}\ln\left(\frac{1+e^{-W_-}}{1+e^{-W_+}}\right)\right.$$
$$+\frac{2T}{k}\sum_{m=1}^{\infty}(-1)^{m+1}\left(\frac{2}{m^3}+\frac{k}{Tm^2}\right)$$
$$\left.\times(e^{-mW_-}-e^{-mW_+})\right]\Theta(k^2-\omega^2)\text{sgn}(\omega),$$
(4.22...)

$$W_\pm = \left|\frac{|\omega|\pm k}{2T}\right|.$$
(4.23)

The first two terms π_0, π_{2P} arise from the process $q\bar{q}\rightarrow\gamma$ and π_{LD} from in-medium bremsstrahlung $q\rightarrow\gamma q$. The long-wavelength limit $k\ll T$ is dominated by π_{LD} and simplifies to the HTL expression Eq. (4.17).

D. Dynamics of the virtual photon cloud

As discussed above, the asymptotic long time limit is determined by the behavior of $\text{Im}\,\Pi_T(k,\omega)$ for $\omega\sim k$, therefore it is convenient to separate the contribution from the positive and negative frequency regions in the integral in Eq. (4.10). Using the properties $\text{Im}\,\Pi_T(k,-\omega)=-\text{Im}\,\Pi_T(k,\omega)$ and $n(-\omega)=-[1+n(\omega)]$ we write

$$\frac{dN(t)}{d^3xd^3k} = \frac{dN^{(+)}(t)}{d^3xd^3k} + \frac{dN^{(-)}(t)}{d^3xd^3k}$$
(4.24)

in terms of the positive $(+)$ and negative $(-)$ frequency contributions respectively, given by

$$\frac{dN^{(+)}(t)}{d^3xd^3k} = \frac{1}{(2\pi)^3k}\int_0^\infty\frac{d\omega}{\pi}n(\omega)\text{Im}\,\Pi_T(k,\omega)$$
$$\times\frac{1-\cos[(\omega-k)(t-t_0)]}{(\omega-k)^2}$$
(4.25)

$$\frac{dN^{(-)}(t)}{d^3xd^3k} = \frac{1}{(2\pi)^3k}\int_0^\infty\frac{d\omega}{\pi}[1+n(\omega)]\text{Im}\,\Pi_T(k,\omega)$$
$$\times\frac{1-\cos[(\omega+k)(t-t_0)]}{(\omega+k)^2}.$$
(4.26)

For further analysis, it is convenient to add together the terms that feature the Bose-Einstein distribution function, thus we write instead,

$$\frac{dN}{d^3xd^3k} = \frac{dN^{(T)}}{d^3xd^3k} + \frac{dN^{(V)}}{d^3xd^3k},$$
(4.27)

with

$$\frac{dN^{(T)}(t)}{d^3xd^3k} = \frac{1}{(2\pi)^3k}\int_0^\infty\frac{d\omega}{\pi}n(\omega)\text{Im}\,\Pi_T(k,\omega)$$
$$\times\left\{\frac{1-\cos[(\omega-k)(t-t_0)]}{(\omega-k)^2}\right.$$
$$\left.+\frac{1-\cos[(\omega+k)(t-t_0)]}{(\omega+k)^2}\right\},$$
(4.28)

$$\frac{dN^{(V)}(t)}{d^3xd^3k} = \frac{1}{(2\pi)^3k}\int_0^\infty\frac{d\omega}{\pi}\text{Im}\,\Pi_T(k,\omega)$$
$$\times\frac{1-\cos[(\omega+k)(t-t_0)]}{(\omega+k)^2}.$$
(4.29)

Both terms are positive, however, while the frequency integral in $dN^{(T)}(t)/d^3xd^3k$ is finite because of the Bose-Einstein distribution function, the frequency integral in $dN^{(V)}(t)/d^3xd^3k$ features divergences associated with the virtual photon cloud, which can be seen as follows.

The contribution $dN^{(V)}(t)/d^3xd^3k$ does not feature resonant denominators, therefore it remains positive and does not grow in time at long time. The oscillatory terms average out on a short time interval, as shown explicitly in Fig. 2 which displays the negative frequency contribution integrated up to a frequency cutoff $\omega_c=100$ GeV.
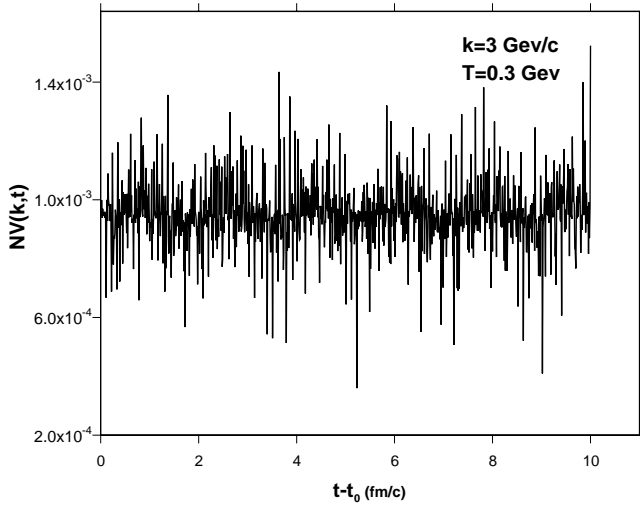
FIG. 2. The contribution $dN^{(V)}(t)/d^3xd^3k$ given by Eq. (4.29) integrated up to $\omega_c = 100$ GeV for $k = 3$ GeV/c; $T = 0.3$ GeV.

Thus, after a very short transient time the average of $dN^{(V)}(t)/d^3xd^3k$ is obtained by neglecting the oscillatory cosine term in Eq. (4.29).

The remaining time independent term in Eq. (4.29) features two distinct contributions:

(i) The zero temperature part of Im Π_T, namely π_0 given by Eq. (4.21) yields the distribution of photons in the *virtual photon cloud of the vacuum* given by

$$\frac{dN_{vv}}{d^3xd^3k} = \frac{1}{k}\int_k^\infty \frac{\pi_0(\omega,k)}{(\omega+k)^2}\frac{d\omega}{8\pi^4}. \qquad (4.30)$$

This contribution can be extracted by taking $T = 0$ and $t_0 \to -\infty$ in $dN(t)/d^3xd^3k$, it is linearly divergent and it clearly must be subtracted since it is not observable.

(ii) The finite temperature contributions from π_{2P} and π_{LD} for $k \gg T$ are dominated by the region $\omega \sim k$ in the frequency integral in Eq. (4.29) which is *finite*. A lengthy but straightforward calculation from Eqs. (4.22) and (4.23) yields the following result for the frequency integral of both these terms for $k \gg T$:

$$\left.\frac{dN^{(V)}(t)}{d^3xd^3k}\right|_{av} - \frac{dN_{vv}}{d^3xd^3k} \simeq \frac{10\alpha_{em}\zeta(3)}{32\pi^4}\frac{T^3}{k^3} + O\left(\frac{1}{k^5}\right) \qquad (4.31)$$

where "av" refers to the time average of the oscillatory term and $\zeta(3) = 1.202057\ldots$. The result (4.31) originates in the region $\omega \sim -k$ both in the Landau damping as well as two particle contribution. This region features a contribution that is not exponentially suppressed in k for $k \gg T$.

It is clear that the integral over the momenta k yields a logarithmically divergent number of photons *in the medium* and a linearly divergent energy integral. We identify this

temperature dependent term as describing the virtual photon cloud *in the medium*, which again must be subtracted since it is unobservable.

The divergence associated with the virtual cloud of the vacuum given by Eq. (4.30) as well as the divergences in the photon number and energy stemming from the Eq. (4.31) must both be subtracted from $dN^{(V)}(t)/d^3xd^3k$.

An alternative and illuminating interpretation of the virtual cloud of the vacuum emerges by noticing that Eq. (4.30) is related with the vacuum wave function renormalization Z given by

$$Z = 1 + \mathrm{Re}\left.\frac{\partial\Pi_0^T(\omega,k)}{\partial\omega^2}\right|_{\omega=k}$$

$$= 1 - \frac{1}{2\pi k}\int_{-\infty}^{+\infty}d\omega'\frac{\mathrm{Im}\,\Pi_T(\omega',k;T=0)}{(k-\omega')^2}, \qquad (4.32)$$

where we used the dispersion relations Eqs. (A6), (A7). We see that Eq. (4.30) is just the zero temperature wave function renormalization to order e^2. The vacuum virtual cloud dresses the bare particles into the physical "in" or "out" states; the wave function renormalization is simply the overlap of these.

The asymptotic reduction formula (LSZ formulation) requires that

$$a_{\mathbf{k},\lambda}; a_{\mathbf{k},\lambda}^\dagger \to Z^{-1/2}a_{\mathbf{k},\lambda;out}; Z^{-1/2}a_{\mathbf{k},\lambda;out}^\dagger. \qquad (4.33)$$

Thus multiplying the number operator by Z^{-1}, cancels the vacuum contribution to $O(e^2)$ thus justifying the subtraction of the vacuum term. The asymptotic reduction (LSZ) formalism requires the *zero temperature* wave function renormalization since the in and out states are the states created from the physical *vacuum* by the in and out operators.

In the *medium* the extra in-medium contribution to the virtual cloud dresses the physical particle into a *quasiparticle*, in this case a plasmon [28,29]; these are not asymptotic states. Thus the time dependent terms which are associated with the virtual cloud at asymptotically long times are actually describing the dynamics of formation of the quasiparticle in the medium.

While subtracting the vacuum term corresponds to multiplying by the inverse of the zero temperature wave function renormalization according to the LSZ reduction formula and the propagation of a physical particle in the out state, a similar interpretation for the medium contribution is not available. The virtual cloud of the medium dresses the physical particle into a quasiparticle as it evolves in the medium but is not an asymptotic state. The subtraction of the in medium virtual cloud cannot be justified on the basis of asymptotic theory.

Furthermore, there is no unambiguous manner to subtract the divergent terms at all times, since the oscillatory terms are finite, and subtracting solely the time independent terms

leaves an expression that becomes negative, features the divergences described above at the initial time $t = t_0$ but is finite for any $t \neq t_0$.

Hence, in this section we proceed to subtract *completely* the contribution $dN^{(V)}(t)/d^3x d^3k$ and use the following definition of the subtracted yield for the analysis that follows:

$$
\frac{dN(t)}{d^3x d^3k} \equiv \frac{dN^{(T)}(t)}{d^3x d^3k}
$$

$$
= \frac{1}{(2\pi)^3 k} \int_0^\infty \frac{d\omega}{\pi} n(\omega) \operatorname{Im} \Pi_T(k, \omega)
$$

$$
\times \left[\frac{1 - \cos(\omega - k)(t - t_0)}{(\omega - k)^2} + \frac{1 - \cos(\omega + k)(t - t_0)}{(\omega + k)^2} \right]. \quad (4.34)
$$

This expression is finite and positive at all time and the large ω, k regions are exponentially suppressed.

We emphasize that completely subtracting $dN^{(V)}(t)/d^3x d^3k$ also neglects the positive and *finite* time dependent contributions from this term but which cannot be unambiguously separated from the divergent terms during a finite time interval.

At asymptotically long time the definition of the yield (4.34) features a term that is constant in time and terms that grow either linearly or logarithmically (or both) in time. The time independent and finite contribution which is typically associated with the virtual photon cloud can be separated unambiguously from the photons produced with a constant rate *only in the asymptotic long time limit*. However, since the QGP has a finite lifetime, only the virtual cloud of the vacuum and the medium contribution that leads to a divergent number of photons and energy can be unambiguously associated with the virtual photon cloud of the medium. Furthermore, these (divergent) contributions are associated with very fast oscillations and become constant in time on a very short time scale ($\ll 1$ fm/c) as clearly shown in Fig. 2.

To be sure, the photons produced by the plasma are detected far away from the collision region and (practically) at infinite time. However, these photons had been *produced* in the plasma during a (much shorter) time scale $t_0 \leq t \leq t_f$ with t_f being the hadronization time. Clearly the vacuum part of the virtual cloud can be recognized and subtracted unambiguously; it is given by Eq. (4.30). However, identifying the contribution to the virtual photon cloud in the medium can only be achieved unambiguously if the formation time of the virtual cloud is much shorter than the lifetime of the QGP and the number of photons in the cloud diverges. As mentioned above, the time dependent terms which asymptotically are associated with the virtual cloud are describing the dynamics of formation of the *quasiparticle* in the medium.

In Sec. V below we will introduce and implement a method that allows to separate the divergent contributions to the virtual cloud which are responsible for the rapid oscillations, in an effective manner.

The contribution $dN^{(T)}(t)/d^3x d^3k$ evolves on longer time scales and contains all of the potentially secular terms, those that grow linearly, logarithmically etc. Furthermore, since the large ω regions are exponentially suppressed, the integrals are dominated by the region $\omega \sim k$ and $\omega \sim 0$. The region $\omega \sim k$ leads to secular terms from the resonant denominators, the nonresonant terms feature oscillations on the time scale $\sim 1/k$, hence their time dependence is relevant during the lifetime of the QGP especially for long wavelengths. Thus, no subtractions on this contribution are warranted.

E. Real time vs S-matrix yields

We can now establish a comparison between the yields and spectra predicted by the real time expression Eq. (4.34) with those obtained from the S-matrix approach (the equilibrium *rate*). The equilibrium *rate* in leading logarithmic order approximation in the strong coupling α_s is given in Ref. [8], and for two flavors (up and down) of quarks (and three colors) becomes

$$
\frac{dN_{SM}}{d^3k d^4x} = \frac{40\pi T^2}{9(2\pi)^3} \alpha_{em} \alpha_s(T) \frac{n_f(k)}{k}
$$

$$
\times \left[\ln\left(\frac{\sqrt{3}}{4\pi\alpha_s(T)} \right) + C_{tot}\left(\frac{k}{T} \right) \right]
$$

$$
C_{tot}(z) = \frac{1}{2} \ln(2z) + \frac{0.041}{z} - 0.3615 + 1.01 e^{-1.35z}
$$

$$
+ \sqrt{\frac{4}{3}} \left[\frac{0.548}{z^{3/2}} \ln\left(12.28 + \frac{1}{z} \right) \right.
$$

$$
\left. + \frac{0.133 z}{\sqrt{1 + \frac{z}{16.27}}} \right], \quad (4.35)
$$

where $n_f(k)$ is the Fermi distribution function. This fit seems to be very accurate in the region of momenta $0.2 \leq k/T \leq 50$ [8].

We will also use the lattice parametrization [30] for the temperature dependence of the strong coupling $\alpha_s(T)$ given by

$$
\alpha_s(T) = \frac{6\pi}{29 \ln \frac{8T}{T_c}}; \quad T_c \sim 0.16 \text{ GeV}. \quad (4.36)
$$

Although this lattice fit is valid at high temperatures and certainly not near the hadronization phase transition, we will assume its validity in the temperature range relevant for RHIC in order to obtain a numerical estimate of the S-matrix yield. We note, however, that at $\alpha_s(0.3 \text{ GeV}) \sim 0.24$ the validity of the perturbative expansion is at best questionable.
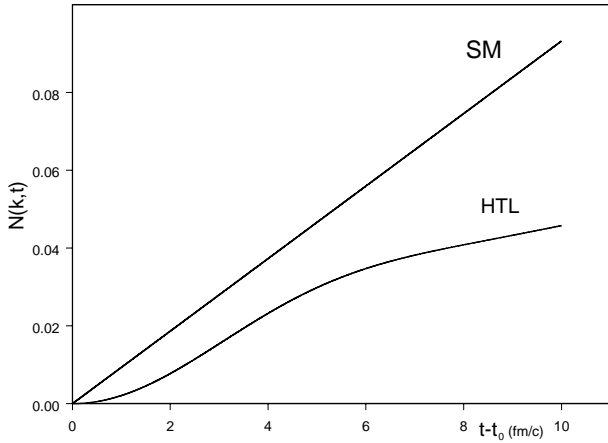
FIG. 3. Comparison between the *S*-matrix yield SM given by Eqs. (4.35)–(4.37) and the real time yield (HTL) given by Eq. (4.19) in the HTL approximation, both for $k=0.1$ GeV; $T=0.5$ GeV as a function of $t-t_0$ (in fm/c). $N(k,t)=d^6N/d^3kd^3x$.

The yield per unit phase space as a function of time obtained from this rate is given by

$$\frac{dN_{SM}(t)}{d^3kd^3x} = (t-t_0)\frac{dN_{SM}}{d^3kd^4x}. \qquad (4.37)$$

We begin by comparing the yield from the real time evolution with the photon polarization in the hard thermal loop approximation, valid for $k \ll T$.

Since the hard thermal loop (HTL) limit Eq. (4.17) is valid for $k \ll T$ and the formula for the rate (4.35) is valid for $0.2 < k/T < 50$ the comparison between the two is reliable for $k/T \sim 0.2$.

A comparison of the yields per unit phase space from the time dependent real time expression (4.10) given by Eq. (4.19) in the HTL approximation, and the leading order result of the *S*-matrix formulation obtained from Eq. (4.35) [8] for $k=0.1$ GeV; $T=0.5$ GeV is displayed in Fig. 3.

It is clear from this figure that during a finite time interval compatible with the expected lifetime of QGP in local thermal equilibrium at RHIC, the hard thermal loop contribution is of the same order as the *S*-matrix result.

Figure 4 compares the real time yield Eq. (4.34) with the full one loop photon polarization given by Eqs. (4.20)–(4.23) to the *S*-matrix yield for $k=3$ GeV/c; $T=0.3$ GeV. The real time yield is dominated by the Landau damping contribution and clearly competes with the *S*-matrix result during the lifetime of the QGP at RHIC.

Figure 5 displays the logarithm of the real-time photon yield given by Eq. (4.28) vs k compared to the *S*-matrix result for $T=0.3$ GeV; $t-t_0=10$ fm/c. Clearly both spectra fall off exponentially, but the spectrum from the real time yield falls off slower and displays an excess of photons as compared to the equilibrium one for $k \gtrsim 2.2$ GeV/c. Since Eq. (4.28) is dominated by the Landau damping contribution to the imaginary part of the photon polarization, these photons originate in bremsstrahlung which is a medium effect.
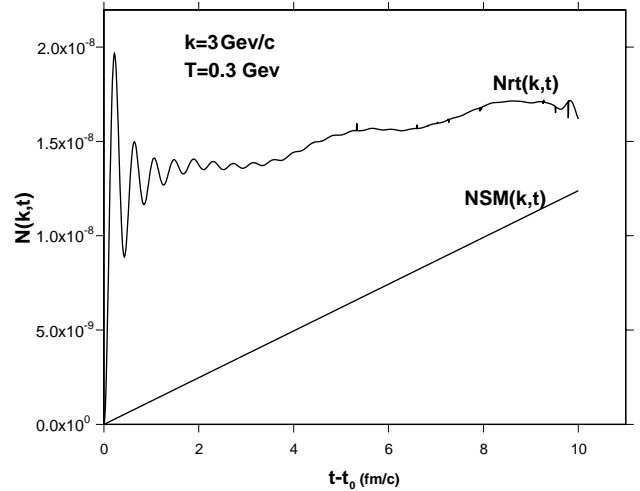

FIG. 4. Comparison between the *S*-matrix yield $N_{SM}(k,t)$ given by Eqs. (4.35)–(4.37) and the real time yield $N_{rt}(k,t)$ given by Eq. (4.34) for $k=3$ GeV/c; $T=0.3$ GeV as a function of $t-t_0$ (in fm/c). The real time yield is dominated by the Landau damping contribution given by Eq. (4.23). $N(k,t)=d^6N/d^3kd^3x$.

We emphasize that we have only considered the contribution from Eq. (4.28) since we have subtracted the full contribution from Eq. (4.29) which is not exponentially suppressed but falls of as a power law. The subtraction of Eq. (4.29) was motivated by the fact that this contribution features both vacuum and in-medium divergences associated with the unobservable virtual photon cloud and the finite contributions cannot be unambiguously separated during a finite interval of time. We will revisit this point in Sec. V below where we introduce a formulation that allows to separate the virtual cloud by allowing an initial preparation stage.

F. Energetics

If the thermalized plasma is emitting photons, the energy radiated away must be drained from the plasma. In this sec-
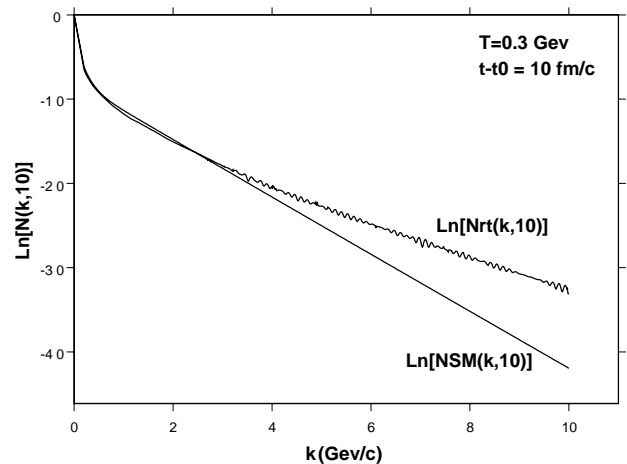

FIG. 5. Comparison of the spectra, $\ln N(k,t)$ vs k between the *S*-matrix N_{SM} and real time N_{rt} yield given by Eq. (4.34) for $T=0.3$ GeV and $t-t_0=10$ fm/c.

tion we study the different contributions to the energy radiated away with the escaping photons. The total energy is conserved, namely

$$\text{Tr}[\rho(t)H] = \text{Tr}[e^{-iH(t-t_0)}\hat{\rho}(t_0)e^{iH(t-t_0)}H]$$

$$= \text{Tr}[\hat{\rho}(t_0)H], \qquad (4.38)$$

where H is the total Hamiltonian (3.13). Passing to the interaction picture of H_0 in Eq. (3.13) the equation above Eq. (4.38) becomes

$$\text{Tr}[\hat{\rho}(t_0)H] = \text{Tr}\{\hat{\rho}_{ip}(t_0)U^{-1}(t,t_0)[H_0 + H_I(t)]U(t,t_0)\}, \qquad (4.39)$$

where $U(t,t_0)$, $H_I(t)$ and $\hat{\rho}_{ip}(t_0)$ are given by Eqs. (3.15) and (3.16) respectively and $U^{-1}(t,t_0) = U(t_0,t)$. Assuming translational invariance in a (large) volume V, the statement of conservation of energy of Eq. (4.39) becomes

$$\Delta\mathcal{E}_{QCD}(t) + \mathcal{E}_\gamma(t) + \mathcal{E}_I(t) = 0, \qquad (4.40)$$

where the second term above corresponds to the energy per unit volume radiated away by the photons produced in the plasma [see Eq. (3.12)] and we have introduced the following definitions:

$$\Delta\mathcal{E}_{QCD}(t) = \frac{1}{V}\text{Tr}[\hat{\rho}_{ip}(t_0)U^{-1}(t,t_0)H_{QCD}U(t,t_0)]$$

$$- \frac{1}{V}\text{Tr}[\hat{\rho}_{ip}(t_0)H_{QCD}], \qquad (4.41)$$

$$\mathcal{E}_\gamma(t) = \int d^3k\, k\, \frac{dN(k,t)}{d^3x\, d^3k}, \qquad (4.42)$$

$$\mathcal{E}_I(t) = \frac{1}{V}\text{Tr}[\hat{\rho}_{ip}(t_0)U^{-1}(t,t_0)H_I(t)U(t,t_0)]. \qquad (4.42)$$

The individual terms above can be computed to lowest order in α_{em} by expanding the time evolution operator up to second order in the interaction. A lengthy but straightforward computation using the initial density matrix given by Eq. (4.1) and introducing an intermediate set of states leads to the following result:

$$\left\{ \begin{array}{c} \Delta\mathcal{E}_{QCD}(t) \\ \mathcal{E}_\gamma(t) \\ \mathcal{E}_I(t) \end{array} \right\}$$

$$= \int \frac{d^3k}{(2\pi)^3} \frac{1}{k} \int_{-\infty}^{+\infty} \frac{d\omega}{\pi} \left\{ \begin{array}{c} -\omega \\ k \\ \omega-k \end{array} \right\} n(\omega)\,\text{Im}\,\Pi_T(\omega,k)$$

$$\times \frac{1-\cos(\omega-k)(t-t_0)}{(\omega-k)^2}, \qquad (4.43)$$

which manifestly satisfies conservation of energy as in Eq. (4.40). The asymptotic long time limit is determined by the region of the spectral density $\omega \sim k$, thus it is clear from the expressions in Eq. (4.43) that the interaction energy shuts-off in the long time limit and for asymptotically long time the rate of radiative energy loss by the photons is balanced by the rate of energy loss of the plasma, which can be interpreted as radiative cooling, namely

$$\frac{d\mathcal{E}_\gamma(t)}{dt} = -\frac{d\mathcal{E}_{QCD}(t)}{dt}. \qquad (4.44)$$

We emphasize that this result is only valid in the long time limit; during a finite time interval there is a contribution from the interaction energy which necessarily is present to satisfy energy conservation.

As discussed in Sec. IV D for the virtual photon cloud, the negative frequency contribution features the zero temperature divergence associated with the virtual photon cloud of the vacuum, as well as the divergence associated with the virtual photon cloud in the medium. The energy in the photon cloud in the vacuum diverges as the fourth power of a cutoff, while the energy in the medium contribution of the virtual cloud diverges linearly with a cutoff since the number of photons diverges only logarithmically, as can be seen from Eq. (4.31). Furthermore since the virtual cloud builds up in a very short time scale, the negative frequency contribution without the Bose-Einstein distribution averages to a time independent constant on a time scale $\ll 1$ fm/c, as can be gleaned from Fig. 2. Since this contribution features the divergences associated with the vacuum and in-medium virtual photon clouds, we subtract it from the energy, consistently with Eq. (4.34).

Therefore we now study the following subtracted energies:

$$\left\{ \begin{array}{c} \Delta\mathcal{E}_{QCD}(t) \\ \mathcal{E}_\gamma(t) \\ \mathcal{E}_I(t) \end{array} \right\}$$

$$= \int \frac{d^3k}{(2\pi)^3} \frac{1}{k} \int_0^\infty \frac{d\omega}{\pi} n(\omega)\,\text{Im}\,\Pi_T(\omega,k)$$

$$\times \left[\left\{ \begin{array}{c} -\omega \\ k \\ \omega-k \end{array} \right\} \frac{1-\cos[(\omega-k)(t-t_0)]}{(\omega-k)^2} \right.$$

$$\left. + \left\{ \begin{array}{c} \omega \\ k \\ -\omega-k \end{array} \right\} \frac{1-\cos[(\omega+k)(t-t_0)]}{(\omega+k)^2} \right]. \qquad (4.45)$$

In subtracting the negative frequency contribution without the Bose-Einstein distribution function, we are also neglect-

ing the *finite* parts of the negative frequency contribution to $\mathcal{E}_\gamma(t)$, which as mentioned above cannot be extracted unambiguously.

Figure 6 displays the subtracted energy radiated in photons [see Eq. (4.45)] as a function of time for $T = 0.3$ GeV as compared to the energy obtained from the S-matrix yield. The real-time energy reveals the logarithmic growth in time and it is of the same order as that obtained from the S-matrix yield during the lifetime of the QGP expected at RHIC.

Figure 7 displays the subtracted contributions Eq. (4.45) to $\Delta \mathcal{E}_{QCD}(t)$ and $\mathcal{E}_I(t)$, as a function of t for $T = 0.3$ GeV.

We confirmed numerically that the main physical mechanism of radiative energy loss is Landau damping by studying separately the different contributions to the photon polarization in the energy.

It is clear from the figure that the interaction term evolves on time scales of order $\sim 7-8$ fm/c, and that the QGP cools by photon emission faster than the change in interaction energy, a clear signal that the photons being emitted are mainly a consequence of the cooling of the QGP. The numerical analysis reveals that the energy in photons grows and that in the QGP diminishes logarithmically, while the interaction energy slowly approaches a constant over the time interval of the same order as the lifetime.

V. MODELLING THE INITIAL STATE: QUASIADIABATIC INTERPOLATING STATES

The expression for the total direct photon yield at a given time t given by Eq. (4.10) was obtained from an initial density matrix corresponding to a QGP in thermal equilibrium and the photon vacuum. The assumption on the photon vacuum is in agreement with the assumption of no photons in the initial state in the S-matrix calculation. The rationale for this choice is that the photons produced from the preequilibrium state leave the system without buildup of the photon population, and the real time calculation described above makes explicit this choice of initial state.

The study of the dynamics of the photon cloud above indicates that a real time description of photon production—a necessary treatment to address the finite lifetime of a QGP—must include the analysis of the virtual photon cloud and a consistent and systematic separation between the contributions from the virtual photon cloud and the observed photons.

The S-matrix formulation bypasses any discussion of the dynamics of the photon cloud by initializing at $t_i \rightarrow -\infty$, taking the final time $t_f \rightarrow +\infty$ and extracting only the contributions that lead to a linear time dependence in the yield. In this manner, all constant contributions, such as that of the photon cloud, as well as those that grow slower than linear in time, are neglected. This can also be summarized with the statement that in the asymptotic long time limit, the yield is independent of the initial conditions. This statement requires that the strong interaction states are in thermal equilibrium from the initial time $t_i \rightarrow -\infty$. As discussed above, this does not apply to a QGP produced from a collision and thermalized at ~ 1 fm/c *after* the collision with a finite lifetime of a few fm/c.
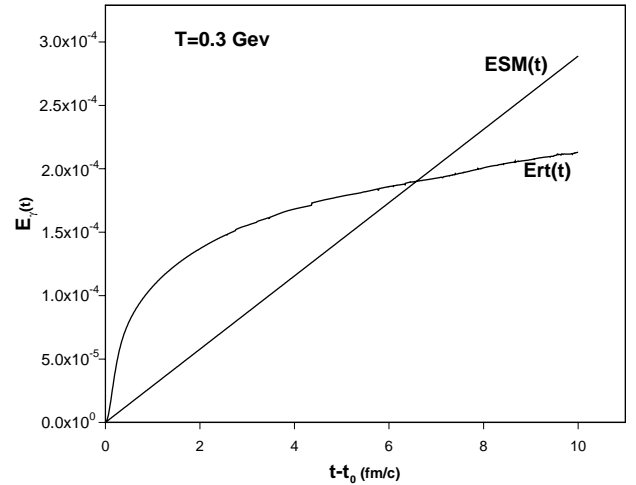

FIG. 6. Comparison between the energy density radiated in photons as a function of time for $T = 0.3$ GeV. The real time energy radiated in photons $E_{rt}(t)$ displays the logarithmic time dependence. The energy obtained from the S-matrix yield is $E_{SM}(t)$.

The detailed analysis of the dynamics of the virtual photon cloud highlights the difficulty and ambiguity in trying to separate the contribution from the virtual photon cloud from the contribution that grows in time during a finite lifetime. In the vacuum the virtual cloud relates the physical to the bare state, thus subtracting the vacuum virtual cloud amounts to studying the propagation of physical photons. However, the virtual cloud in the medium dresses a physical particle into a *quasiparticle*, hence the time dependent terms associated with the in-medium virtual cloud are actually describing the dynamics of formation of a plasmon quasiparticle.

In Sec. IV D we analyzed the formation of the virtual photon cloud, and recognized that the negative frequency contribution features divergences associated with the virtual cloud of the vacuum as well as of the medium. Clearly these divergences are unobservable and must be subtracted, leaving solely finite contributions to the real time yield.

The subtraction of the divergences associated with the virtual cloud is ambiguous during a finite time interval and we *defined* the real time yield by Eq. (4.34) to include only the positive and negative frequency contributions that are suppressed by the Bose-Einstein distribution function. Such definition leads to a finite and manifestly positive photon number density, but is not the only possible definition.

In particular the subtraction (4.30) of the virtual photon cloud of the vacuum, namely the $T = 0$ contribution to the photon yield, entails that the quarks are asymptotic states in the infinite past and the photon cloud was built up during the evolution of these asymptotic states from $t_i \rightarrow -\infty$ up to the collision time. However, this assumption does not correspond to the actual QGP physics.

Before the collision, quarks and gluons must be described as partons confined inside the nuclei and in terms of their distribution functions. Associated with the charged partons there is a photon cloud with a distribution function that depends on the charged parton distribution function in the nuclei.

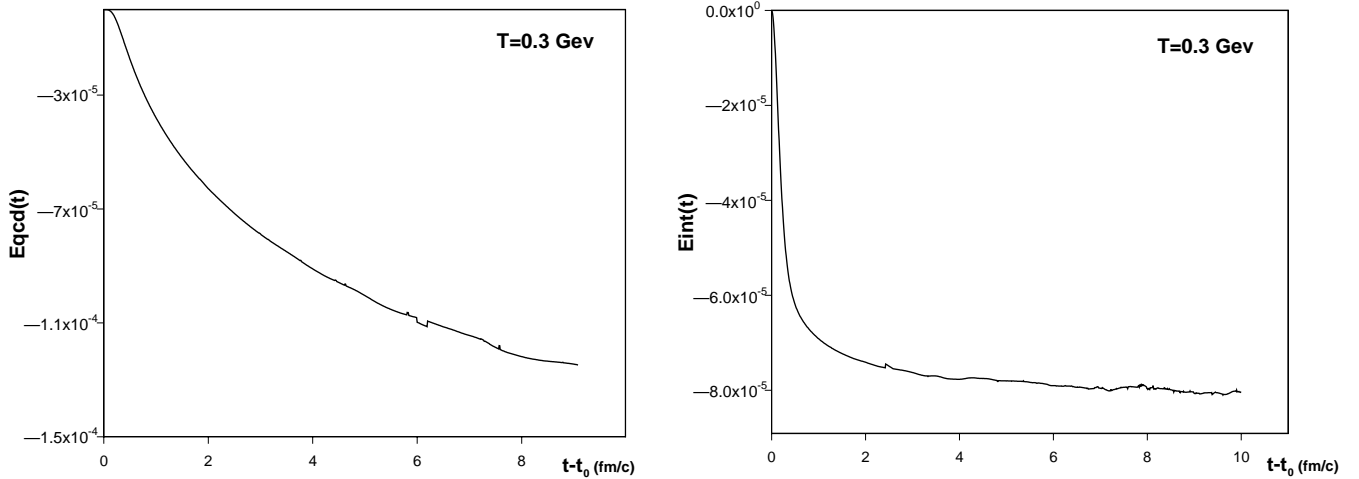What happens to this photon cloud during and after the

FIG. 7. Positive frequency contribution to $\Delta\mathcal{E}_{QCD}(t)$ (left panel) and $\mathcal{E}_I(t)$ (right panel) vs $t-t_0$ for $T=0.3$ GeV.

collision? Obviously this question is very difficult to address quantitatively, however the following are some possibilities [32].

(i) The photon cloud is shaken-off by the collision resulting in a flash of photons during the preequilibrium stage. These photons have a different origin from those being emitted from parton-parton annihilation or bremsstrahlung discussed in Ref. [24]. If the photon cloud is shaken off after the collision, it will form again during the time between the collision and the thermalization of the plasma ~ 1 fm/c because of the electromagnetic interaction.

(ii) The partons deconfine during the collision becoming free and the photon cloud is not modified either by the deconfinement or by the parton-parton rescattering that leads to a thermalized QGP.

Clearly which of these (or other) possibilities describes the actual physics of the collision cannot be assessed with the current level of theoretical understanding.

The importance of these questions cannot be underestimated. If the lifetime of the QGP were truly infinite, the photon yield at long times would be insensitive to the initial conditions and the contribution to the total yield from the initial stage will be of $O(1/t)$. However, given the short lifetime of the QGP, the initial condition not only is important but it bears an imprint in the spectrum. During the finite lifetime of the plasma there is no clear and unambiguous separation between the photons produced at a constant rate, those that are produced at a slower rate and those that are associated with the virtual photon cloud in the *asymptotic long time limit*.

Although a detailed understanding of these issues is lacking, we can provide an approximate description that will model the essential ingredients. Thus, we now modify the choice of the initial density matrix in order to account for a period of electromagnetic dressing of the strong interaction eigenstates during the preequilibrium stage between the collision and the onset of thermalization.

For this purpose, we now revisit the Gell-Mann-Low theorem [31] that obtains the exact eigenstates of the total Hamiltonian from the free field *in* states in terms of the adia-

batic Møller wave operator. Define the Møller wave operator

$$U_\epsilon(0,-\infty)=\text{T}\exp\left[-i\int_{-\infty}^{0}e^{\epsilon t}H_I(t)dt\right], \qquad (5.1)$$

where $H_I(t)$ is the interaction Hamiltonian in the interaction picture of H_0. The Gell-Mann-Low theorem asserts that if the states $|n\rangle$ are eigenstates of the Hamiltonian H_0, then the states

$$\widetilde{|n\rangle}=U_\epsilon(0,-\infty)|n\rangle, \qquad (5.2)$$

are eigenstates of the full Hamiltonian H. The Møller wave operator adiabatically dresses the noninteracting bare state to be the full interacting dressed state during an infinite period of time. If quarks and gluons were truly asymptotic states the process of scattering, thermalization and photon emission would indeed be consistent with the dressing of the bare states from the infinite past. However, quarks and gluons are not asymptotic states, furthermore the actual collision involves bound states of quarks and gluons which are liberated after the nucleus-nucleus collision but the adiabatic hypothesis is not suitable to describe the process of formation or break up of bound states. Namely, the adiabatic hypothesis which is the basis of the S-matrix approach is not suitable to describe the dynamics of confinement and deconfinement.

If partons are freed after the collision, the dressing process has to take place during the preequilibrium stage either completely, if in the process of the collision the partons shed their virtual cloud, or partially if the virtual cloud of photons that partons carried as bound states is also carried after the collision. This discussion brings to the fore the difficulty in separating unambiguously the virtual cloud from the observable photons during a finite lifetime, and manifestly makes clear the inadequacy of the S-matrix approach to describe any physical process in a QGP of a finite lifetime.

Given that there is no current understanding of these issues, we now provide an approximate description of the dressing between the time of collision and the onset of local thermodynamic equilibrium.

For this purpose, we define the interaction picture (with respect to H_0) *quasiadiabatic interpolating states* up to lowest order in the electromagnetic coupling as

$$|n_q;\gamma\rangle = \left[1 - i \int_{-\infty}^{t_0} e^{\Gamma(t-t_0)} H_I(t)dt + O(e^2)\right]|n_q\rangle \otimes |0_\gamma\rangle. \tag{5.3}$$

The physical interpretation of these states is that the electromagnetic interaction dresses the eigenstates H_0 during a time scale Γ^{-1}. A natural time scale to describe the preequilibrum stage, between the collision and termalization is about 1 fm/c.

These states interpolate between the exact *in* states when $\Gamma \to 0^+$ and the eigenstates of H_0 for $\Gamma \to +\infty$. We note that these are entangled states in the sense that they are not simple tensor products of QCD and photon states, therefore these initial states are correlated.

We can now construct an initial density matrix at time t_0 in terms of these states that is reminiscent of a thermal density matrix but in terms of the dressed states (5.3), namely

$$\hat{\rho}_{ip}^\Gamma(t_0) = \sum_{n_q} e^{-\beta E_{n_q}} |n_q;\gamma\rangle\langle n_q;\gamma|. \tag{5.4}$$

The interpretation of this initial density matrix is that the QCD eigenstates have been dressed by the electromagnetic interaction on a time scale $1/\Gamma$ which describes the time between the collision and the onset of thermalization.

It is important to note that this initial density matrix *does not* describe a state of thermal equilibrium under the strong interactions because it *does not* commute with H_{QCD} since the quark electromagnetic current that enters in the definition of the dressed states does not commute with H_{QCD}.

We highlight this important point: *any* initial density matrix that includes the photon cloud, a result of the electromagnetic interaction *does not* commute with H_{QCD}, hence it cannot describe a state in thermodynamic equilibrium under the strong interactions. The only manner to construct an initial density matrix *with* photons in the initial state and in thermal equilibrium under the strong interactions is for this density matrix to be factorized into a tensor product of a density matrix of pure QCD and a density matrix of free photons. The density matrix given by Eq. (4.1) is one such (the simplest) case.

Once the initial density matrix (5.4) is specified, its time evolution is completely determined by the full Hamiltonian and given by Eq. (3.17). The evolution of the number operator in time is therefore given by Eq. (3.18), which upon inserting a complete set of eigenstates of H_0 leads to the following result:

$$\frac{dN^\Gamma(t)}{d^3x d^3k} = \frac{1}{(2\pi)^3 k} \int_{-\infty}^{+\infty} \frac{d\omega}{2\pi} \text{Im} \, \Pi_T(k,\omega) n(\omega)$$

$$\times \left[\frac{1}{\Gamma^2 + (\omega-k)^2} + \frac{2\Gamma^2}{\Gamma^2 + (\omega-k)^2} \right.$$

$$\times \frac{1 - \cos(\omega-k)(t-t_0)}{(\omega-k)^2}$$

$$\left. + \frac{2\Gamma}{\Gamma^2 + (\omega-k)^2} \frac{\sin(\omega-k)(t-t_0)}{(\omega-k)} \right]. \tag{5.5}$$

The expression Eq. (5.5) clearly coincides with Eq. (4.10) in the $\Gamma \to +\infty$ limit. In the opposite limit $\Gamma \to 0^+$ it becomes

$$\frac{dN^\Gamma(t)^{t_i \to -\infty}}{d^3x d^3k} = \frac{1}{(2\pi)^3 k} \left\{ \frac{\text{Im} \, \Pi_T(k,\omega=k)}{e^{k/T}-1}(t-t_i) \right.$$

$$\left. + \int \frac{d\omega}{\pi} \frac{\text{Im} \, \Pi_T(k,\omega)}{e^{\omega/T}-1} \mathcal{P} \frac{1}{(\omega-k)^2} \right\}. \tag{5.6}$$

Thus, in the limit $\Gamma \to 0^+$ the yield agrees with Eq. (4.12) when the initial time t_0 is taken to $-\infty$ and the photoproduction rate coincides with the result from the S-matrix calculation, as it must be.

Furthermore, using the identity Eq. (4.11), the long time limit $t - t_0 \to +\infty$ yields,

$$\frac{dN^\Gamma(t)^{t-t_0 \to -\infty}}{d^3x d^3k} = \frac{1}{(2\pi)^3 k} \left\{ \frac{\text{Im} \, \Pi_T(k,\omega=k)}{e^{k/T}-1}[t-t_0+\Gamma^{-1}] \right.$$

$$\left. + \int \frac{d\omega}{\pi} \frac{\text{Im} \, \Pi_T(k,\omega)}{e^{\omega/T}-1} \mathcal{P} \frac{1}{(\omega-k)^2} \right\}. \tag{5.7}$$

Since Γ^{-1} is the time scale between the collision and the onset of thermalization, Eq. (5.7) coincides with the S-matrix calculation in the long time limit from the instant of the collision. Therefore, this initial preparation is a physically acceptable description insofar as it reproduces the asymptotic long time limit.

We note that Eq. (5.5) does not vanish at $t = t_0$ because of the first term in the bracket, which is time independent. The value of the photon yield (5.5) at $t = t_0$, namely the contribution determined by the first term in the bracket in Eq. (5.5), can be interpreted as the total number of photons (per unit phase space) created during the time scale Γ^{-1}. These photons correspond to the virtual cloud as well as the observable photons emitted during the preequilibrium stage. This is precisely the physics that the density matrix in terms of the quasiadiabatic states is meant to describe.

This interpretation becomes clear in the limit $\Gamma \to 0$ in which case

$$\frac{1}{\Gamma^2+(\omega-k)^2} \overset{\Gamma\to 0}{=} \pi\Gamma^{-1}\delta(\omega-k)+\mathcal{P}\frac{1}{(\omega-k)^2}+O(\Gamma).$$

(5.8)

The principal part leads to the divergences associated with the virtual cloud and since Γ^{-1} is the time scale of preparation, the term with the delta function gives the real photons produced during the time scale Γ^{-1}.

We then subtract the time independent term (first in the bracket) in Eq. (5.5) (which does not contribute to the rate). We thus define a photon number that vanishes at the initial time t_0 and that is independent of the initial photon cloud, namely

$$\frac{dN_S(t)}{d^3xd^3k}=\frac{1}{(2\pi)^3k}\int_{-\infty}^{+\infty}\frac{d\omega}{\pi}\frac{\operatorname{Im}\Pi_T(k,\omega)}{e^{\omega/T}-1}\frac{\Gamma}{\Gamma^2+(\omega-k)^2}$$

$$\times\left[\Gamma\frac{1-\cos[(\omega-k)(t-t_0)]}{(\omega-k)^2}\right.$$

$$\left.+\frac{\sin[(\omega-k)(t-t_0)]}{\omega-k}\right].$$

(5.9)

The interpretation of this definition is gleaned from the expression

$$\frac{dN_S(t)}{d^3xd^3k}=\int_{t_0}^{t}dt'\frac{dN^\Gamma(t')}{d^3xdt'd^3k},$$

(5.10)

with $dN^\Gamma(t)/d^3xd^3k$ given by Eq. (5.5). Thus, the subtracted number is obviously the photon yield between the time at which the plasma is thermalized t_0 (after the collision) and the time t. Hence, this definition neglects the virtual photon cloud in the initial state and assumes that the observable photons produced during the preequilibrium stage leave the plasma.

The extra powers of $\omega-k$ in the denominator in Eq. (5.9) render the total yield *finite*.

The subtraction of the time independent term in Eq. (5.5) has accounted for the divergent contributions of the virtual cloud of the vacuum and the medium, leaving a *finite* result for the time dependent yield.

Therefore, this initial preparation and the subtraction of the total photon number at the time of thermalization, provide a possible systematic framework to approximate the physics of the initial state.

In order to assess the (finite) contribution of the virtual cloud, it proves convenient again to separate the positive and negative frequency contributions. We then obtain

$$\frac{dN_S(t)}{d^3xd^3k}=\frac{dN_S^{(T)}(t)}{d^3xd^3k}+\frac{dN_S^{(V)}(t)}{d^3xd^3k}$$

(5.11)

with

$$\frac{dN_S^{(T)}(t)}{d^3xd^3k}=\frac{1}{(2\pi)^3k}\int_0^\infty\frac{d\omega}{\pi}\operatorname{Im}\Pi_T(k,\omega)n(\omega)$$

$$\times(\mathcal{T}^+[\omega,k,t-t_0]+\mathcal{T}^-[\omega,k,t-t_0])$$

(5.12)

$$\frac{dN_S^{(V)}(t)}{d^3xd^3k}=\frac{1}{(2\pi)^3k}\int_0^\infty\frac{d\omega}{\pi}\operatorname{Im}\Pi_T(k,\omega)\mathcal{T}^-[\omega,k,t$$

$$-t_0],$$

(5.13)

in terms of the functions

$$\mathcal{T}^\pm(\omega,k,t-t_0)=\frac{\Gamma}{\Gamma^2+(\omega\mp k)^2}\left[\Gamma\frac{1-\cos[(\omega\mp k)(t-t_0)]}{(\omega\mp k)^2}\right.$$

$$\left.+\frac{\sin[(\omega\mp k)(t-t_0)]}{\omega\mp k}\right].$$

(5.14)

The term $dN_S^{(V)}(t)/d^3xd^3k$ includes the vacuum contribution given by $\pi_0(\omega,k)$ in $\operatorname{Im}\Pi_T(k,\omega)$. However, now this vacuum contribution is *finite* but of order Γ^2/k^2 thus leading to a divergent number of photons which must be identified with a vacuum contribution to the virtual cloud and must therefore be subtracted.

The remaining term

$$\frac{dN_{VS}^{(V)}(t)}{d^3xd^3k}=\frac{1}{(2\pi)^3k}\int_0^\infty\frac{d\omega}{\pi}[\pi_{2P}(\omega,k)$$

$$+\pi_{LD}(\omega,k)]\mathcal{T}^-[\omega,k,t-t_0],$$

(5.15)

is finite and only depends on the medium.

A lengthy but straightforward analysis of the time average (neglecting the oscillatory functions) yields the following result valid in the limit $k\gg T,\Gamma$

$$\frac{1}{(2\pi)^3k}\int_0^\infty\frac{d\omega}{\pi}\frac{\Gamma^2[\pi_{2P}(\omega,k)+\pi_{LD}(\omega,k)]}{\Gamma^2+(\omega+k)^2}$$

$$\simeq\frac{10\alpha_{em}\zeta(3)}{32\pi^4}\frac{T^3\Gamma^2}{k^5},$$

(5.16)

plus terms that are exponentially suppressed for $k\gg T$. Thus, the total yield, and the energy radiated in photons are *finite*.

Figure 8 shows the vacuum subtracted term $dN_{VS}^{(V)}(t)/d^3xd^3k$ for two values of the momentum for a range of parameters expected at RHIC.

Comparing Fig. 8 with Fig. 2 it becomes clear that the oscillations in Fig. 8 are on much longer time scales, in particular it can be gleaned from Fig. 8 that the *shortest* oscillation time scale is of $O(1/k)$ and that there are longer
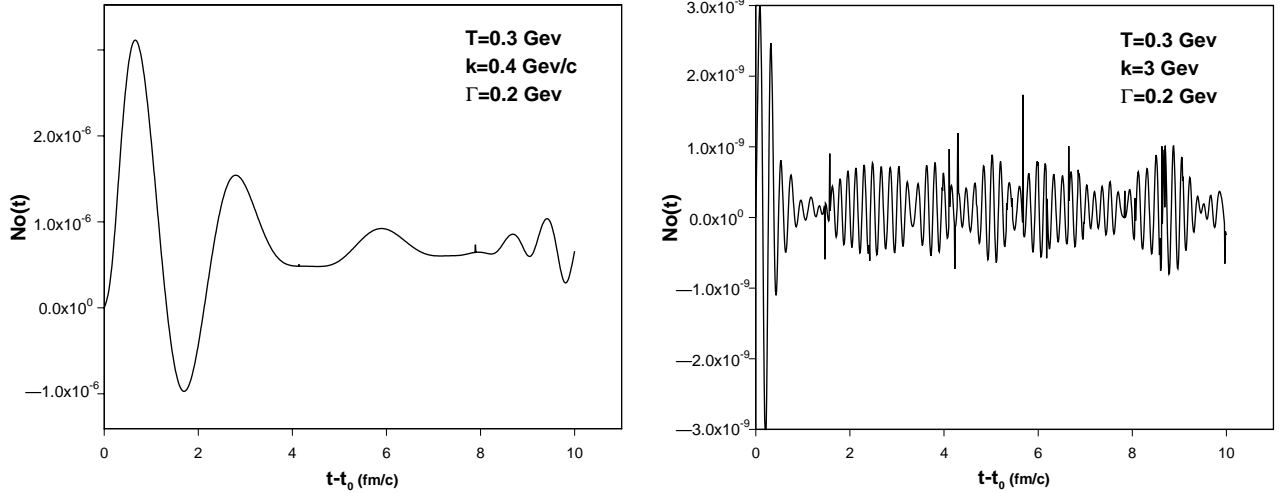
FIG. 8. The contribution of Eq. (5.15) for $k=0.4$ GeV/c (left panel), $k=3$ GeV/c (right panel) for $\Gamma=0.2$ GeV; $T=0.3$ GeV.

time scales. While the results leading to Fig. 2 are sensitive to the cutoffs because the integrals diverge, leading to very rapid oscillations, the frequency integral in Eq. (5.15) is finite and the integrand falls off fast. Hence, the oscillations are not sensitive to large frequencies and are on time scales which are of the order of the lifetime of the QGP.

Thus, the contribution given by Eq. (5.15) is (i) finite and leads to a finite photon number and energy, (ii) the real time dynamics is on time scales of the order of the QGP, certainly at least for $0 \leq k \leq 2-3$ GeV/c. Therefore there is *a priori* no reason to subtract this term from the yield and it must be considered on equal footing as the contribution from Eq. (5.12).

Thus, the final expression for the photon yield with initial preparation on a time scale Γ^{-1} and after subtracting the virtual cloud and the preequilibrium yield is given by

$$\frac{dN_F(t)}{d^3x d^3k} = \frac{1}{(2\pi)^3 k} \int_0^\infty \frac{d\omega}{\pi} \{ \mathrm{Im}\,\Pi_T(k,\omega) n(\omega) \mathcal{T}^+[\omega,k,t-t_0]$$

$$+ [\mathrm{Im}\,\Pi_T(k,\omega)[1+n(\omega)]$$

$$- \mathrm{Im}\,\Pi_T(k,\omega;T=0)] \mathcal{T}^-[\omega,k,t-t_0]\}, \qquad (5.17)$$

where $\mathcal{T}^\pm[\omega,k,t-t_0]$ are given by Eq. (5.14). This expression is one of the *main* results of this study.

While we obtained this expression based on the analysis of the lowest order contribution, we advocate Eq. (5.17) to lowest order in α_{em} and *all orders* in α_s as an *effective* description of the photoproduction yield during a finite time interval. This expression includes the initial state preparation and has the following important properties:

(i) The divergences associated with the virtual photon cloud both in the vacuum and in the medium, as well as the photons produced during the initial stage prior to thermalization are subtracted.

(ii) The total yield as well as the energy are finite.

(iii) The limit $t-t_0 \rightarrow +\infty$ correctly reduces to the photon production rate obtained from the S-matrix calculation.

(iv) The limit $\Gamma \rightarrow 0$ also leads to the S-matrix result for the rate. This is expected because $\Gamma \rightarrow 0$ corresponds to an infinitely long preparation stage, which implies an infinitely long time interval, for which the S-matrix calculation applies.

(v) The initial preparation time scale Γ^{-1} is a *parameter* that describes in an effective manner the time scale between the collision and the onset of the QGP in LTE. It can be used as a fitting parameter for phenomenological purposes.

Figure 9 displays the yield given by Eq. (5.17) for several values of the initial preparation time scale for values of k,T for which the HTL approximation is valid. As mentioned before, the HTL approximation gives the leading contribution for $k \ll T$ and does not depend on the vacuum contribution.

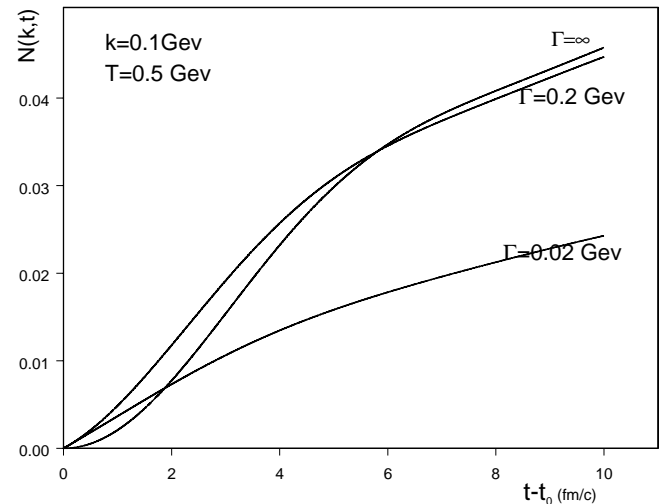The values $\Gamma=0.2$ GeV correspond to a time scale of

FIG. 9. Comparison between the real time yield with initial preparation given by Eq. (5.17) for $k=0.1$ GeV; $T=0.5$ GeV as a function of $t-t_0$ (in fm/c) in the HTL approximation Eq. (4.17).
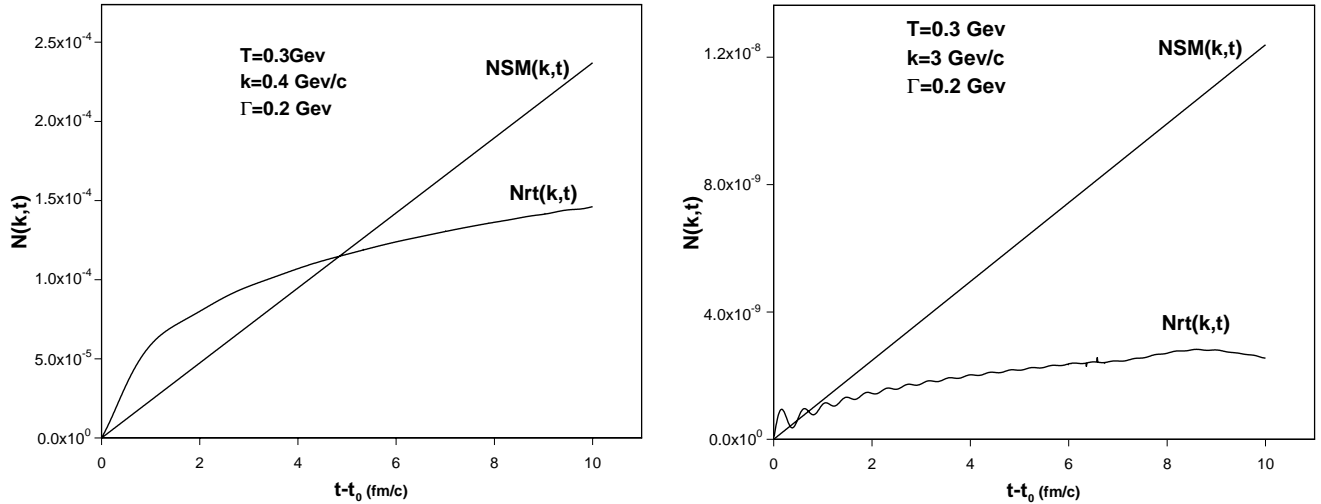
FIG. 10. Comparison between the real time yield $N_{rt}(t)$ with initial preparation given by Eqs. (5.17) with $\Gamma = 0.2$ GeV; $T = 0.3$ GeV and the S-matrix yield as a function of $t - t_0$ (in fm/c) for $k = 0.4$ GeV (left panel) and $k = 3$ GeV (right panel).

about 1 fm/c which describes the time scale between the collision and the onset of a thermalized QGP. It is clear from the figure that change in the yield is rather minor for long-wavelength photons even in the case of an extremely long preparation time scale. Thus for $k \ll T$ the real time yield from the lowest order $O(\alpha_{em} \alpha_s^0)$ is of the same order as the S-matrix yield during the lifetime of the QGP and is rather insensitive to the preparation time scale.

Figure 10 shows the comparison between the real time yield with the full one-loop photon polarization [Eqs. (4.20)–(4.23)] and the S-matrix yield as a function of time for a preparation time scale 1 fm/c for $k = 0.4, 3$ GeV; $T = 0.3$ GeV. Comparing the right panel of Fig. 10 to the case $\Gamma = \infty$ displayed in Fig. 4 we see that they are qualitatively similar, with the quantitative difference in the overall scale. However, it is clear from these figures that the yield from the real time calculation from processes that do not contribute to the S-matrix rate, is of the same order of or larger than the yield obtained from the S-matrix expression during the lifetime of the QGP.

To emphasize this point further for larger values of the momentum, Fig. 11 displays the real time yield for $k = 3$ GeV/c; $T = 0.3$ GeV for a wide range of the time scale for initial preparation.

It is clear from this figure that while there are a few quantitative changes with respect to the case $\Gamma = \infty$, qualitatively the results are similar and all of the same order.

Figure 12 shows the spectrum of photons produced during the lifetime of the QGP expected at RHIC ~ 10 fm/c for a preparation time scale of 1 fm/c and $T = 0.3$ GeV. The left panel compares the real time and S-matrix yields vs k. The right panel displays the logarithm of the yield vs the logarithm of the wave vector for the real time case only and clearly displays the power law fall of $\sim k^{-5}$ for large momenta ($k \gg T, \Gamma$) as predicted by Eq. (5.16). These figures suggest a crossover from an exponential to a power law fall in the spectrum of the real time yield, the crossover occurring at a value k_c which depends on Γ. We find numerically

that for $\Gamma \sim 0.2$ GeV, $k_c \approx 2.7 - 3$ GeV/c resulting in a marked flattening of the spectrum. We also find numerically that k_c decreases upon increasing Γ. The power law dominance is a telltale of the contribution of the term in the real time yield Eq. (5.17) that does not feature a Bose-Einstein distribution function which leads to an exponential suppression. As discussed above, this power law leads to a finite number of photons and a radiated energy. In the infinite time limit the contribution that leads to this power law would be identified with the *finite* distribution of photons in the virtual cloud, but as analyzed and discussed in detail above, during the finite lifetime this term cannot be separated from the other contributions and enters in the yield on the same footing.

Thus, the power law spectrum at large momentum is a hallmark of the processes that contribute during the finite lifetime of the QGP and that cannot be captured by the S-matrix approach.
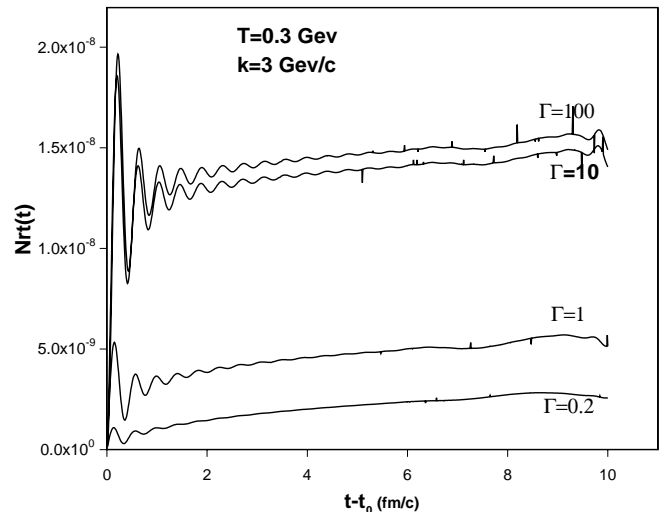

FIG. 11. Comparison between the real time yield $N_{rt}(t)$ with initial preparation given by Eqs. (5.17) for several values of Γ, for $k = 3$ GeV/c; $T = 0.3$ GeV.
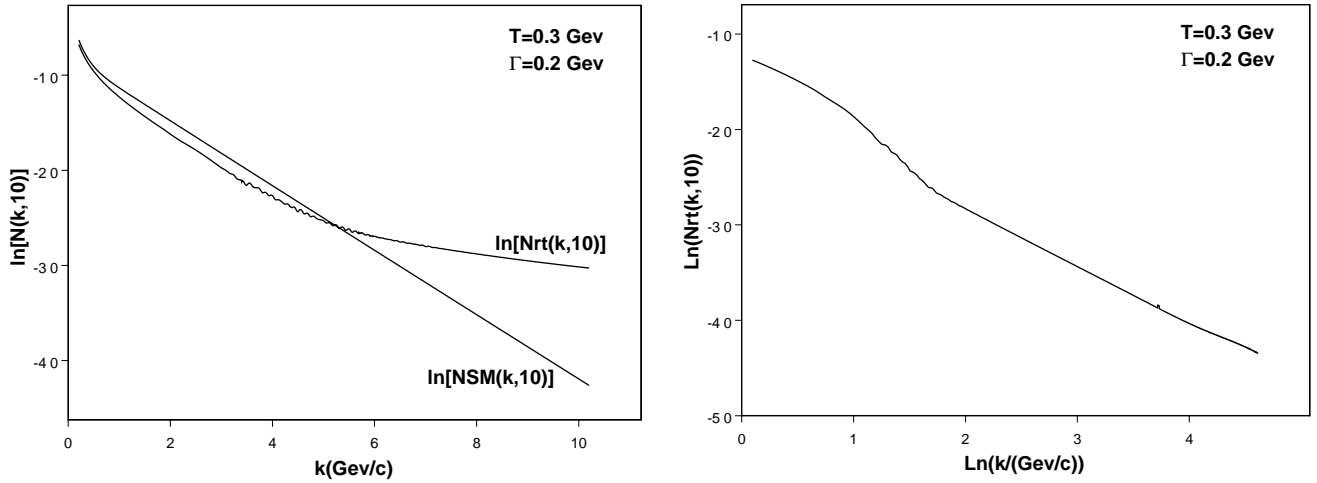
FIG. 12. Comparison between the logarithms of the real time yield $\ln N_{rt}(k,t)$ with initial preparation given by Eqs. (5.9) with $\Gamma = 0.2$ GeV and the S-matrix yield $\ln N_{SM}(k,t)$ as a function of k (in GeV/c) for $T = 0.3$ GeV.

We have also studied the energy [see Eqs. (4.41), (4.42)], which results in expressions similar to those given by Eq. (4.45) but the positive and negative frequency contributions are replaced by those in the subtracted yield (5.17). The numerical study of the energy reveals minor quantitative changes with respect to the results shown in Figs. 6 and 7. The contributions of the terms which are not exponentially suppressed by the Bose-Einstein distribution function begin to become important when the momentum is of order $k \sim 3 - 4$ GeV/c at which point all contributions are very small. The momentum integrals that lead to the energies are dominated by momenta $\lesssim 1.5 - 2$ GeV/c for $\Gamma \sim 0.2$ GeV. Consequently, the results for the energies from the initial density matrix with the initial stage preparation are very similar to the results displayed in Figs. 6 and 7 with an overall small change in the scale.

VI. CONCLUSIONS, DISCUSSIONS AND IMPLICATIONS

In this article we studied the direct photon production from a QGP in local thermodynamic equilibrium during a finite lifetime. After discussing the shortcomings of the usual approach based on the S-matrix calculation of the emission *rate*, we focused on describing photon production directly from the real time evolution of an initial density matrix.

The main premise of this study is that there are processes that contribute to the direct photon yield during the finite lifetime of the QGP but that are *not* captured by the S-matrix approach. We highlighted this point by restricting our study to the lowest order contribution of $O(\alpha_{em})$ to the yield. While this contribution is subleading in the asymptotic long time limit (that is if the QGP were truly a stationary state of infinite lifetime) it does contribute to the yield during a finite lifetime.

We began our study by first considering an initial density matrix that describes a QGP in LTE with no photons in the initial state, compatible with all of the assumptions in the literature that lead to the S-matrix calculations of the emission rate. This study revealed the important aspect of the dynamics of formation and build-up of the virtual photon cloud. We highlighted that the finite lifetime of the transient QGP results in that the photon spectrum retains information of the initial state and pointed out the inherent ambiguities associated with the separation of the virtual and observable photons during the short time scale between formation and hadronization.

While the terms that yield divergences in the number of photons and energy from the virtual photon cloud of the vacuum and in the medium can be identified, there is no unambiguous manner to subtract these from the finite contributions during a finite lifetime. Within this choice of initial state, we *defined* the yield subtracting the divergent contributions associated with the virtual clouds but also finite, time dependent terms because there is no unambiguous manner to extract these. The resulting yield clearly shows that there are contributions from processes that cannot be captured by the S-matrix approach, but that contribute to the direct photon yield during the finite lifetime.

In particular, within the assumption of no initial photons, our study revealed that even after subtracting finite contributions, the yield from lowest order processes is of the same order of *or larger* than those obtained in the S-matrix calculations.

We then provided an effective description of the preparation of the initial state by constructing the initial density matrix of a thermalized QGP in terms of quasiadiabatic states obtained by electromagnetic dressing the QCD eigenstates over a time scale Γ^{-1}. This time scale describes in an effective manner the preequilibrium stage between the deconfinement of partons and the onset of a thermalized QGP; it is expected to be of the order of 1 fm/c. This quasiadiabatic initial condition on the density matrix allows to extract the (divergent) contribution from the virtual cloud built-up as well as the observable photons emitted during the preequilibrium stage. The main result of this analysis is Eq. (5.17) which provides an effective but systematic formulation of direct photon production from a QGP in local thermal equilibrium directly in real time. There are many advantages of this formulation over the usual S-matrix approach: (i) it does

not suffer from the caveats associated with the S-matrix approach described in Sec. II; (ii) it describes photon production in real time as an initial value problem, consistently with hydrodynamics [20]; and (iii) it includes a description of the initial state in an effective manner in terms of the parameter Γ which is associated with the inverse of the time scale between the collision and that of thermalization.

This *is* the time scale during which partons are almost free and parton-parton scattering brings the deconfined partons to a state of local thermodynamic equilibrium.

The final expression for the real time photon yield given by Eq. (5.17) has several important properties:

(i) It reproduces the result of the S-matrix result in the two limits in which it must be equivalent: the $t - t_0 \rightarrow +\infty$ and the $\Gamma \rightarrow 0$ limits. Both limits actually refer to a QGP of infinite lifetime, for which the S-matrix calculation applies.

(ii) It allows to separate the divergent contributions from the vacuum as well as the in-medium virtual cloud, along with the observable photons produced during the preequilibrium stage. Therefore this expression leads to a finite photon yield and a total finite radiated energy.

(iii) This description parametrizes the initial state in terms of a time scale Γ^{-1}, which is a phenomenological parameter. Namely it provides an effective description of the physics between the time at which nucleus-nucleus collision results in deconfined quarks and gluons and the time at which a QGP in LTE emerges.

A. Phenomenological consequences

The main results of this study point out that during the finite lifetime of a QGP in LTE expected at RHIC or LHC there are processes that contribute to the yield that are not captured by the usual S-matrix approach. While we have focused on the lowest order such term, there are already many important consequences of phenomenological relevance:

(i) The correct direct photon yield is actually *larger* than that calculated with the S-matrix approach. This is a consequence of the processes that contribute even at lowest order, and also processes missed by the S matrix that arise from the region of $\omega \neq k$ in the imaginary part of the photon polarization. Thus, the correct photon yield will be larger than the current estimates. A reliable estimate of the correction calls for a recalculation of the imaginary part of the photon polarization for all $\omega \neq k$ up to $O(\alpha_s \ln(1/\alpha_s))$. Such calculation is currently not available.

(ii) An important telltale of the processes that contribute to the yield during a finite lifetime is a *power law* spectrum of the yield of the form k^{-5}. The coefficient of the power law bears information on the temperature as well as the time scale for thermalization Γ^{-1} of the plasma. This telltale is in striking contrast with the S-matrix yield which features an exponential fall-off. Depending on the value of the time scale Γ^{-1} this power law sets in for $k_c \gtrsim 3$ GeV/c with $k_c \sim 3$ GeV/c for $\Gamma^{-1} \sim 1$ fm/c. While this power law spectrum may be an important signature, it sets in for a region of momenta in which a description of the QGP in LTE may break down. As mentioned above, the current data on the

elliptic flow parameter $v_2(p_T)$ [14,23] reveal large departures from hydrodynamics (+pQCD) which relies on a QGP in LTE for $p_T > 2$ GeV/c. In the region of momentum up to ~ 2 GeV/c the real time yield is almost indistinguishable from an exponential fall off, but begins to flatten towards the power law at about ~ 3 GeV/c. It is possible that the excess of photons and the flattening of the spectra in the WA98 data [13] may be explained by the processes studied here and that originate in the finite lifetime of a QGP.

B. More questions

Our study indicates that direct photons from a QGP in LTE may not be a clean signature of the formation and evolution of the plasma as originally envisaged. The short transient nature of the QGP entails that the spectrum carries information on the initial, preequilibrium stage. However the electromagnetic properties of the initial state are largely unknown. The current estimates of the *rate* extracted from S-matrix calculations, which assume the existence of asymptotic states, and infinite QGP lifetime are not completely reliable, in particular, these are based on a weak coupling expansion in terms of α_s but at the energy density conjectured to be achieved at RHIC $\alpha_s \sim 0.24$. Hence the estimates based on the S-matrix yield are at best qualitative. During the finite lifetime of the QGP, processes that are completely neglected by the S-matrix approach give contributions to the yield that are of the same order as those of the equilibrium calculations, or even larger at large momenta, since the spectrum from the real time description features a power law fall off $\sim k^{-5}$ versus the exponential fall off of the equilibrium yield.

Thus, in order to provide a phenomenologically reliable estimate the following questions would need to be addressed:

(i) What actually happens to the virtual cloud of photons after the collision? Are the virtual photons in the nuclei shaken off and if so does this result in a flash of photons during preequilibrium?

(ii) The real time yield is sensitive to the structure of the photon polarization for $\omega \neq k$. What is the full expression of the imaginary part of the photon polarization up to $O(\alpha_{em} \alpha_s \ln(1/\alpha_s))$?

(iii) What is the range in momenta (k_T) for which emission from a hydrodynamically expanding QGP is reliable? If the data on elliptic flow for charged particles are extrapolated to photons (and in principle there is no reason to assume otherwise) then the local equilibrium description may only be valid up to $k_T \sim 2$ GeV/c.

(iv) We have discussed above that the terms that are identified with the virtual photon cloud in the medium asymptotically at long time are actually providing *dynamical* information on the formation of the *quasiparticle* in the medium. This is an aspect that has not been explored before; the formation of a quasiparticle in the medium does *not* require scattering and is to lowest order is independent of the mean free path. This can be understood simply from the fact that the HTL approximation does lead to a plasmon quasiparticle but without collisional damping. Namely, the (transverse) plasmon is a consequence of Landau damping and not of any

on-shell scattering process associated with a collisional width or a mean free path. As the produced photon traverses the medium it must necessarily carry with it a polarization of the medium that dresses the photon into a quasiparticle. What happens to this induced polarization once the plasma hadronizes? Is the virtual photon cloud of the QGP released in a flash during the hadronization transition? If so a power fall off $\sim k^{-3}$ in the spectrum is an unavoidable consequence of the formation and later dissipation of the virtual cloud in the medium.

(v) We have studied the consequences of the finite lifetime to lowest order in the perturbative expansion corresponding to the one loop polarization. However for T/T_c between 1 and 3, lattice data clearly show that the quark-gluon plasma is not free or weakly interacting. Thus the next step in the program will consider self-energy and vertex corrections mediated by gluons, namely to higher order in α_s. The strategy will be to compute the photon polarization including higher order corrections in α_s and input its imaginary part in the final equation (5.17). We expect to report on this study soon.

(vi) As we discussed above in Sec. II (see the discussion under "caveats") the elliptic flow data suggest that the hydrodynamic description is not valid for (transverse) momenta $k_T > 2$ GeV/c. Thus the assumption of LTE upon which all calculations of direct photon production from a QGP hinge, including the real time formulation studied in this article, will not be warranted for large momenta. However, and perhaps more importantly, at large transverse momenta it is expected that prompt photons produced during the preequilibrium stage during the pQCD parton-parton scattering will provide a large contribution to the total photon yield. Thus, as stated in Ref. [9], the interpretation of the photon spectrum for large k_T cannot be unambiguous. The current understanding of prompt photon production during preequilibrium is based on parton cascade calculations [24] which invoke a transport description and includes collisions via pQCD parton scattering cross sections. Such an approach implicitly (and explicitly in the collision term) relies on an S-matrix description of the parton-parton collisions and is thus subject to a similar criticism described in Sec. II above. Therefore a reliable estimate of the photon yield for large momenta requires understanding the dynamics beyond LTE and providing a reliable estimate of prompt photons from the preequilibrium stage.

The experimental importance of electromagnetic probes of the QGP warrants a deeper study and assessment of these questions and in our view a reevaluation of the current theoretical status on hard probes.

APPENDIX: PHOTON POLARIZATION TENSOR

The retarded photon polarization tensor is given by

$$\Pi_{ij,ret}(\vec{x}-\vec{x}',t-t')$$
$$= -ie^2\langle[J_i(\vec{x},t),J_j(\vec{x}',t')]\rangle\Theta(t-t'). \quad (A1)$$

Introducing a complete set of simultaneous eigenstates of H_{QCD} and the total momentum operator $\vec{P}$ following the steps described in Sec. IV A above, we find

$$\langle J_i(\vec{x},t)J_j(\vec{x}',t')\rangle$$
$$= \int d^3p\,d\omega\, e^{-i\vec{p}\cdot(\vec{x}-\vec{x}')+i\omega(t-t')}\sigma_{ij}^{>}(\vec{p},\omega),$$
$$(A2)$$

$$\langle J_j(\vec{x}',t')J_i(\vec{x},t)\rangle$$
$$= \int d^3p\,d\omega\, e^{-i\vec{p}\cdot(\vec{x}-\vec{x}')+i\omega(t-t')}\sigma_{ij}^{<}(\vec{p},\omega),$$
$$(A3)$$

where $\sigma_{ij}^{>}(\vec{p},\omega)$ is given by Eq. (4.5) and

$$\sigma_{ij}^{<}(\vec{p},\omega) = \sum_{n_q,m_q} e^{-\beta E_{m_q}}\langle n_q|J_i(\vec{0},0)|m_q\rangle\langle m_q|J_j(\vec{0},0)|n_q\rangle$$
$$\times \delta^3(\vec{p}-\vec{p}_{n_q}+\vec{p}_{m_q})\delta(\omega-E_{n_q}+E_{m_q})$$
$$= e^{\beta\omega}\sigma_{ij}^{>}(\vec{p},\omega). \quad (A4)$$

Introducing the Fourier representation of $\Theta(t-t')$ we find the photon polarization tensor to be given by

$$\Pi_{ij,ret}(\vec{x}-\vec{x}',t-t')$$
$$= \int \frac{d^3p}{(2\pi)^3}\frac{dp_0}{2\pi} e^{-i\vec{p}\cdot(\vec{x}-\vec{x}')}e^{ip_0(t-t')}\Pi_{ij,ret}(\vec{p},p_0),$$
$$(A5)$$

$$\Pi_{ij,ret}(\vec{p},p_0) = (2\pi)^3\int_{-\infty}^{+\infty}d\omega\,\frac{\sigma_{ij}^{>}(\vec{p},\omega)[1-e^{\beta\omega}]}{\omega-p_0+i0}.$$
$$(A6)$$

Therefore the result,

$$(2\pi)^3\sigma_{ij}^{>}(\vec{p},p_0) = \frac{1}{\pi}\frac{\operatorname{Im}\Pi_{ij,ret}(\vec{p},p_0)}{e^{\beta p_0}-1}. \quad (A7)$$

We note that $\operatorname{Im}\Pi_{ij,ret}(\vec{p},p_0)$ is an odd function of p_0 with $\operatorname{Im}\Pi_{ij,ret}(\vec{p},p_0>0)>0$ therefore $\sigma_{ij}^{>}(\vec{p},p_0)>0$ for *all* values of p_0.

[1] E.L. Feinberg, Nuovo Cimento Soc. Ital. Fis., A **34A**, 391 (1976); E. Shuryak, Phys. Lett. **78B**, 150 (1978); B. Sinha, *ibid.* **128B**, 91 (1983).

[2] L.D. McLerran and T. Toimela, Phys. Rev. D **31**, 545 (1985).

[3] J.I. Kapusta, P. Lichard, and D. Seibert, Phys. Rev. D **44**, 2774 (1991); **47**, 4171 (1993).

[4] C. Gale and J.I. Kapusta, Nucl. Phys. **B357**, 65 (1991).

[5] R. Baier, H. Nakkagawa, A. Niégawa, and K. Redlich, Z. Phys. C **53**, 433 (1992).

[6] P.V. Ruuskanen, in *Particle Production in Highly Excited Matter*, Vol. 303 of NATO Advanced Study Institute Series B: Physics, edited by H.H. Gutbrod and J. Rafelski (Plenum, New York, 1992).

[7] P. Aurenche, F. Gelis, R. Kobes, and H. Zaraket, Phys. Rev. D **58**, 085003 (1998).

[8] P. Arnold, G.D. Moore, and L.G. Yaffe, J. High Energy Phys. **12**, 009 (2001).

[9] T. Renk, Phys. Rev. C **67**, 064901 (2003).

[10] J. Alam, S. Sarkar, T. Hatsuda, T.K. Nayak, and B. Sinha, Phys. Rev. C **63**, 021901 (2001); J. Alam, S. Sarkar, P. Roy, T. Hatsuda, and B. Sinha, Ann. Phys. (N.Y.) **286**, 159 (2001).

[11] T. Peitzmann and M.H. Thoma, Phys. Rep. **364**, 175 (2002).

[12] F.D. Steffen, nucl-th/9909035; F.D. Steffen and M. Thoma, Phys. Lett. B **510**, 98 (2001).

[13] WA98 Collaboration, M.M. Aggarwal *et al.*, Phys. Rev. Lett. **85**, 3595 (2000); nucl-ex/0006007.

[14] P. Jacobs, "Measurements of High Density Matter at RHIC," talk presented at the 2002 Slac Summer Institute Topical Conference, hep-ex/0211031.

[15] K. Geiger, Phys. Rep. **258**, 237 (1995); X.-N. Wang, *ibid.* **280**, 287 (1997).

[16] FOPI Collaboration, F. Rami *et al.*, Phys. Rev. Lett. **84**, 1120 (2000).

[17] C.Y. Wong, Phys. Rev. C **48**, 902 (1993); M.G.H. Mostafa and C.Y. Wong, *ibid.* **51**, 2135 (1995).

[18] S. Sarkar *et al.*, J. Phys. G **22**, 951 (1996).

[19] D. Anchishkin, V. Khryapa, and V. Ruuskanen, "Thermal Dilepton Radiation from Finite Fireball," hep-ph/0210346.

[20] D. Boyanovsky and H.J. de Vega, Phys. Rev. D **59**, 105019 (1999); D. Boyanovsky, H.J. de Vega, and S.-Y. Wang, *ibid.* **61**, 065006 (2000); S.-Y. Wang, D. Boyanovsky, H.J. de Vega, and D.-S. Lee, *ibid.* **62**, 105026 (2000); S.-Y. Wang and D. Boyanovsky, *ibid.* **63**, 051702(R) (2001); Nucl. Phys. **A699**, 819 (2002).

[21] J.D. Bjorken, Phys. Rev. D **27**, 140 (1983).

[22] J.-P. Blaizot and J.-Y. Ollitrault, in *Quark-Gluon Plasma 1*, edited by R.C. Hwa (World Scientific, Singapore, 1990).

[23] Star Collaboration, C. Adler *et al.*, Phys. Rev. Lett. **90**, 032301 (2003).

[24] D.K. Srivastava and K. Geiger, Phys. Rev. C **58**, 1734 (1998).

[25] J. Sollfrank, P. Huovinen, M. Kataja, P.V. Ruuskanen, M. Prakash, and R. Venugopalan, Phys. Rev. C **55**, 392 (1997).

[26] D.K. Srivastava and B. Sinha, Phys. Rev. Lett. **73**, 2421 (1994); Phys. Rev. C **64**, 034902 (2001); D.K. Srivastava, Eur. Phys. J. C **10**, 487 (1999).

[27] D. Boyanovsky and H.J. de Vega, "Dynamical Renormalization Group Approach to Relaxation in Quantum Field Theory," Ann. Phys. (N.Y.) (to be published), hep-ph/0302055.

[28] E. Braaten and R.D. Pisarski, Nucl. Phys. **B337**, 569 (1990); **B339**, 310 (1990); R.D. Pisarski, Physica A **158**, 146 (1989); Phys. Rev. Lett. **63**, 1129 (1989); Nucl. Phys. **A525**, 175 (1991).

[29] M. Le Bellac, *Thermal Field Theory* (Cambridge University Press, Cambridge, England, 1996).

[30] F. Karsch, Z. Phys. C **38**, 147 (1988).

[31] M. Gell Mann and F. Low, Phys. Rev. **84**, 350 (1951).

[32] We thank Yuri Dokshitzer for discussions on these issues.